Regeneration of transzonal projections and growth of bovine oocytes in vitro

伏井，実穂子

(Degree)
博士（農学）

(Date of Degree)
2023-03-25

(Date of Publication)
2025-03-25

(Resource Type)
doctoral thesis

(Report Number)
甲第8660号

(URL)
https://hdl.handle.net/20.500.14094/0100482408

博士論文

Regeneration of transzonal projections and growth of bovine oocytes *in vitro*

Transzonal projection の再形成とウシ卵母細胞の体外発育に関する研究

令和 5 年 1 月

神戸大学大学院農学研究科

Mihoko FUSHII

伏井 実穂子

Index

Abbreviations

AI-TI: anaphase I and telophase I

BAM: binary alignment/map

BMP15: bone morphogenetic protein 15

BSA: bovine serum albumin

CC: cumulus cell

cGMP: cyclic guanosine monophosphate

CORO6: coronin 6

DAAM1: dishevelled associated activator of morphogenesis 1

DAPI: 4',6-diamidino-2-phenylindole

DEG: differentially expressed gene

DO: denuded oocyte

ECM: extracellular matrix

ED: early diakinesis

FBS: fetal bovine serum

FC: filamentous chromatin

FDR: false discovery rate

FSCN1: fascin actin-bundling protein 1

FSH: follicle-stimulating hormone

GC: granulosa cell

GDF9: growth differentiation factor 9

GO: gene ontology

GVI–IV: germinal vesicle I–IV

HEPES-199: HEPES-buffered medium 199

LD: late diakinesis

LH: luteinizing hormone

MGC: mural granulosa cell

MI: metaphase I

MII: metaphase II

MYO10: myosin heavy chain 10

NPPC: natriuretic peptide precursor type C

NPR2: natriuretic peptide receptor 2

OCC: oocyte-cumulus cell complex

OCGC: oocyte-cumulus cell-mural granulosa cell complex

OGC: oocyte-granulosa cell complex

PBS: phosphate-buffered saline

PCA: principal component analysis

PGC: primordial germ cell

PVA: polyvinyl alcohol

PVP: polyvinylpyrrolidone

rhFSH: recombinant human follicle-stimulating hormone

RNA-seq: RNA sequencing

SC: stringy chromatin

SCMC: subcortical maternal complex

SKAP2: src kinase associated phosphoprotein 2

TLE6: TLE family member 6, subcortical maternal complex member

TMM: trimmed mean of M values

TPM: transcripts per kilobase million

***t*-SNE:** *t*-distributed stochastic neighbor embedding

TZP: transzonal projection

αMEM: α-minimum essential medium

CHAPTER I

General introduction

Oogenesis is the process of the differentiation, growth, and maturation of oocytes. In mammals, oogenesis starts in the embryonic stage (Saitou and Yamaji, 2012; Saitou and Miyauchi, 2016; Nagaoka and Saitou, 2017). Primordial germ cells (PGCs), which are the primary cells in oogenesis, migrate through the hindgut endoderm toward the genital ridges. After migration, PGCs are then called oogonia, and they undergo proliferation by mitotic division and form oocyte cysts (Tam and Snow, 1981; Pepling and Spradling, 1998). The oogonia subsequently undergo meiotic divisions, then they are called oocytes, and become arrested at the diplotene stage of prophase I of meiosis.

When individual oocytes are surrounded by a single layer of granulosa cells (GCs), primordial follicles are formed (Fig. 1). The origin of GCs has not been determined, however, recently they are speculated to be derived from the ovarian surface epithelium (Hummitzsch *et al*., 2013, 2015). When oocytes start to grow, the surrounding GCs alter their morphology from squamous to cuboidal shape. GCs are promoted to proliferate and survive by follicle-stimulating hormone (FSH) which is secreted from the anterior pituitary. As oocytes grow and GCs proliferate, follicles develop into primary, secondary, and antral follicles (Matzuk *et al*., 2002; Edson *et al*., 2009). After antrum formation, GCs differentiate into cumulus cells (CCs) and mural granulosa cells (MGCs). CCs surround the oocyte directly, while MGCs line the basement membrane of the antral follicle wall. During the follicle development, bovine oocytes grow from 30 μm to 120–125 μm, and acquire meiotic competence (Fair *et al*., 1995; Hyttel *et al*., 1997). After reaching the final size, oocytes are induced to resume meiosis upon the luteinizing hormone (LH) surge, and mature to metaphase II before subsequent ovulation and fertilization.

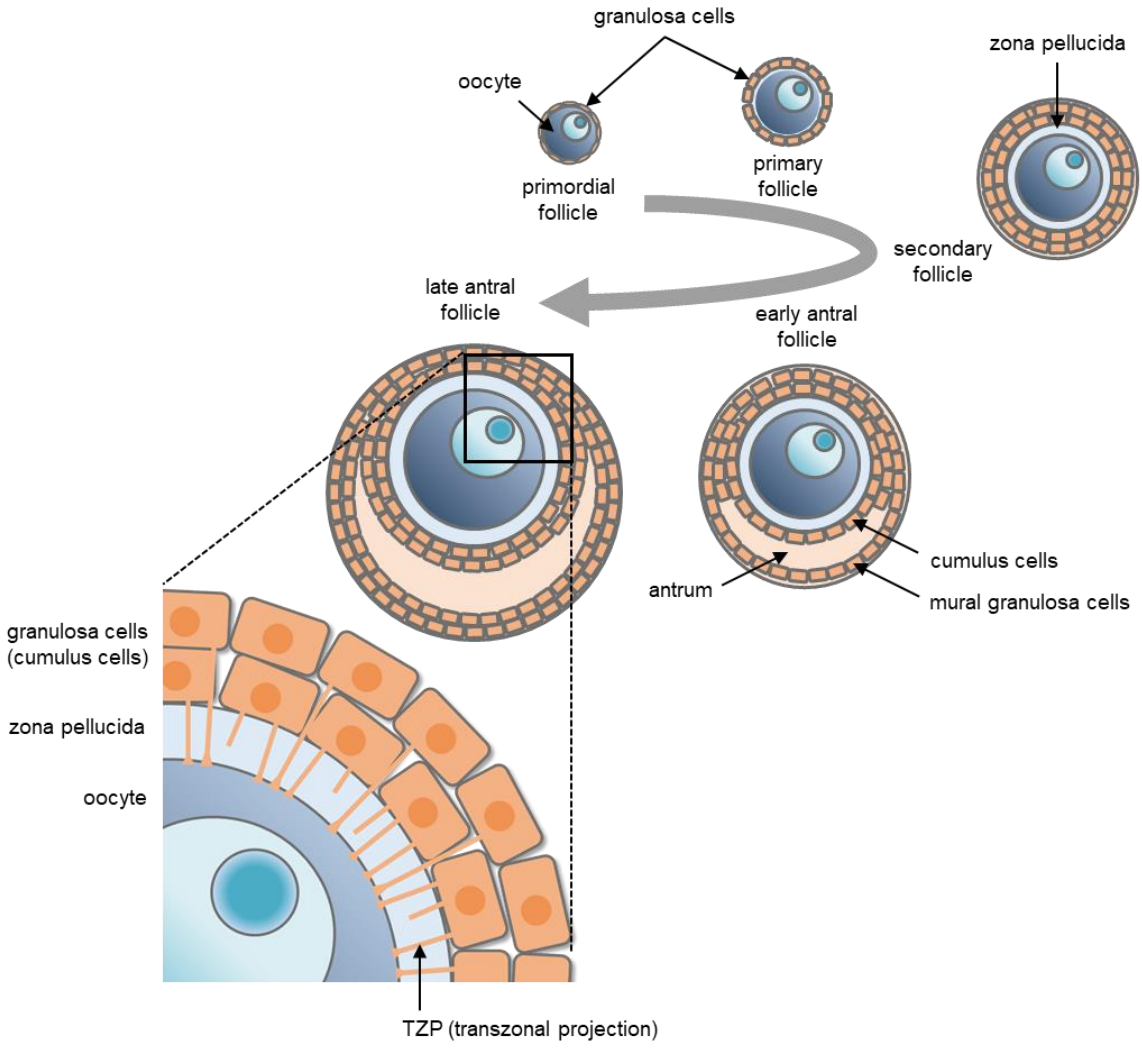

Figure 1 Follicle development and oocyte growth in the ovary. In primordial follicles, oocytes are surrounded by a single layer of squamous granulosa cells (GCs). When oocytes start to grow, the surrounding GCs alter their morphology from squamous to cuboidal shape, and the zona pellucida is formed around the oocytes. GCs extend transzonal projections (TZPs) penetrating the zona pellucida to maintain contact with the oocytes. As oocytes grow and GCs proliferate, follicles develop into primary, secondary, and antral follicles. After antrum formation, GCs differentiate into cumulus cells (CCs) and mural granulosa cells (MGCs). During the follicle development, bovine oocytes grow from 30 μm to 120–125 μm.

For oocyte growth, bidirectional communication between oocytes and GCs or CCs through paracrine signaling and gap junctions is essential (Eppig, 2001; Matzuk *et al*., 2002; Veitch *et al*., 2004; Teilmann, 2005). During the follicle development and oocyte growth, the zona pellucida is formed around the oocytes (Clarke, 2018a, 2018b, 2022), and GCs extend transzonal projections (TZPs) penetrating the zona pellucida to maintain contact with the oocytes (Fig. 1). Oocyte-derived factors regulate the metabolic cooperativity with GCs and CCs by mediating processes such as glycolysis, amino acid uptake, and cholesterol biosynthesis, which are not accomplished by the oocyte alone (Eppig *et al*., 2005; Su *et al*., 2008, 2009). Pyruvate, amino acids, and nucleotides are transported to the oocytes *via* gap junctions at the end of the TZPs (Clarke, 2018a, 2018b, 2022). Although gap junctions permit the transfer of ions and small molecules (< 1 kDa) between cells (Simon and Goodenough, 1998), large molecules such as mRNA and fatty acid binding proteins remain within TZPs (Macaulay *et al*., 2014; Collado *et al*., 2017). Some studies observed membrane vesicles between the oolemma and CC membranes (Macaulay *et al*., 2014, 2016), suggesting that several molecules are transported by these extracellular vesicles at the end of the TZPs (Clarke, 2018a, 2018b, 2022; Muñoz *et al*., 2022).

To understand the mechanism of oocyte growth and to utilize potential sources of oocytes in the ovary, several *in vitro* growth culture systems have been developed. In mice, Eppig and O'Brien (1996) succeeded in the complete oocyte growth from primordial follicles using the combination of *in vitro* organ (ovary) culture and oocyte-granulosa cell complex (OGC) culture methods, and produced offspring from these *in vitro*-grown oocytes. Hikabe *et al*. (2016) reported the reconstitution of the entire process of oogenesis from mouse pluripotent stem cells by reaggregating with embryonic ovarian somatic cells. Furthermore, using mouse embryonic stem cells, Yoshino *et al*. (2021) produced ovarian somatic cells which were able to support oocyte production. They also succeeded in the production of offspring from pluripotent stem cell-derived oocytes (Hikabe *et al*., 2016; Yoshino *et al*., 2021). In large animals, cattle are the only

mammalian species in which offspring have been produced from *in vitro*-grown oocytes (Yamamoto *et al.*, 1999; Hirao *et al.*, 2004; Huang *et al.*, 2016); however, the oocytes were collected from early antral follicles in these studies. In the systems, the maintenance of functional interactions between oocytes and GCs, and the formation of antrum-like structures seem to be the keys to success in growth of oocytes (Hirao, 2012; Makita and Miyano, 2014).

The purpose of the present study was to clarify the ability of CCs or MGCs alone to support bovine oocyte growth *in vitro* with a particular focus on the formation of antrum-like structures and the generation of TZPs. In Chapter II, I examined whether CCs alone would support *in vitro* growth of bovine oocytes from early antral follicles (0.5–0.7 mm in diameter). Additionally, the effect of FSH on oocyte-cumulus cell complex (OCC) development was assessed. In Chapter III, I confirmed the disappearance of TZPs by denudation of oocytes, and the regeneration of TZPs during the coculture of TZP-free denuded oocytes (DOs) with MGCs from early antral follicles. In addition, the effects of FSH on the reconstruction of complexes and the regeneration of TZPs were also examined. Finally, in Chapter IV, I examined whether GCs from secondary follicles and MGCs from late antral follicles were able to reconstruct complexes with TZP-free DOs and regenerate TZPs similar to MGCs from early antral follicles. Furthermore, to confirm that the regenerated TZPs were functional, the development of reconstructed complexes and oocyte growth in the complexes were examined. Then, the transcriptome was analyzed among GCs, CCs, and MGCs collected from secondary, early antral, and late antral follicles.

CHAPTER II

Oocyte growth and antrum formation in oocyte-cumulus cell complexes

Introduction

A wide range of approaches has been developed for *in vitro* growth of bovine oocytes (Hirao and Miyano, 2014). To sustain an appropriate association between oocytes and somatic cells during long-time *in vitro* growth culture, follicles and oocyte-cumulus cell-mural granulosa cell complexes (OCGCs) from early antral follicles around 0.5 mm in diameter have been cultured in collagen gel matrices (Harada *et al*., 1997; Yamamoto *et al*., 1999; Senbon and Miyano, 2002). This culture system maintains the 3-D structure of follicles and OCGCs. However, because collagen gel matrices deteriorate gradually, this procedure is not suitable for long-term culture. Then, Hirao *et al*. (2004) proposed a novel culture system in which OCGCs were cultured with a high concentration of polyvinylpyrrolidone (PVP; molecular weight of 360,000) on the insert membrane. In this system, cultured complexes formed dome-like structures similar to follicular antra (Hirao *et al*., 2004; Makita and Miyano, 2014, 2015). These antrum-like structures are thought to create a suitable microenvironment for oocyte growth (Hirao, 2012; Makita and Miyano, 2014).

The culture medium for oocyte growth has also been improved (Hirao, 2011). Supplementation of hypoxanthine in a culture medium maintained meiotic arrest and provided a better oocyte survival rate (Harada *et al*., 1997; Senbon and Miyano, 2002). Makita and Miyano (2014) demonstrated that a combination of steroid hormones, 17β-estradiol and androstenedione, maintained the structure of the complexes and promoted complete growth and acquisition of meiotic competence in more than half of the cultured bovine oocytes. Some studies have reported the production of offspring from *in vitro*-grown bovine oocytes (Yamamoto *et al*., 1999; Hirao *et*

al., 2004; Huang *et al*., 2016). In large animals, cattle are the only mammalian species in which offspring have been produced from *in vitro*-grown oocytes.

In studies related to *in vitro* growth of bovine oocytes, OCGCs have been used as culture materials to prevent the migration of GCs away from the oocytes and to maintain the proper association between oocytes and GCs during long-term growth culture period, especially on a flat substratum (Hirao *et al*., 2004; Hirao, 2012). However, in studies regarding *in vitro* oocyte maturation and *in vitro* embryo production, OCCs that have no MGCs have been widely used instead of OCGCs. Some studies reported that bovine OCCs collected from early antral follicles (1.2–1.8 mm) (Alam *et al*., 2018a) and porcine OCCs collected from early antral follicles (1.2–1.5 mm) (Morikawa *et al*., 2021, 2022) formed small antrum-like structures during growth culture, and the oocytes in OCCs grew after 5 days. Since the culture systems for bovine oocyte growth have been improved as mentioned above, it will be possible to use bovine OCCs from small antral follicles as the culture materials for oocyte growth.

In this chapter, I aimed to determine whether CCs alone would support the growth of bovine oocytes from early antral follicles (0.5–0.7 mm in diameter). I also assessed the effect of FSH on OCC development. FSH is known to promote GC proliferation *in vivo* and *in vitro* (Hulshof *et al*., 1995; Wandji *et al*., 1996; Harada *et al*., 1997; Gutierrez *et al*., 1997; McLaughlin *et al*., 2010). OCCs were cultured with various concentrations of FSH for 14 days, and the integrity and antrum formation by OCCs were compared. After 14 days, the diameter and meiotic competence of oocytes in cultured OCCs were examined.

Materials and methods

Chemicals

All chemicals were purchased from Sigma-Aldrich (St. Louis, MO, USA) unless otherwise mentioned.

Collection of OCCs

OCGCs were collected from bovine early antral follicles as described previously (Makita and Miyano, 2014), and OCCs were prepared from OCGCs. Briefly, bovine ovaries were obtained from a local slaughterhouse and transported to the laboratory. Ovaries were washed once with 0.2% (w/v) cetyltrimethylammonium bromide (FUJIFILM Wako Pure Chemical Corporation, Osaka, Japan) and three times with Dulbecco's phosphate-buffered saline (PBS) containing 0.1% (w/v) polyvinyl alcohol (PVA) (PBS-PVA). Ovarian cortical slices were collected using a surgical blade (No. 21; ELP, Akiyama-seisakusyo, Tokyo, Japan) and forceps. Early antral follicles (0.5–0.7 mm in diameter) were dissected from ovarian cortical slices in 25 mM HEPES (Dojindo Laboratories, Kumamoto, Japan)-buffered medium 199 (Nissui Pharmaceutical, Tokyo, Japan) (HEPES-199) containing 0.1% (w/v) PVA, 0.85 mg/mL sodium bicarbonate (FUJIFILM Wako Pure Chemical Corporation), and 0.08 mg/mL kanamycin sulfate. The follicles were opened using a surgical blade (No. 10; Feather Safety Razor, Tokyo, Japan) and forceps to collect OCGCs containing growing oocytes. To prepare OCCs, MGCs were removed from the OCGCs as much as possible using a narrow pipette. The resulting complexes, composed of growing oocytes surrounded by two or three layers of CCs, are referred to as OCCs hereafter. The diameter of oocytes (excluding the zona pellucida) in OCCs was measured to the nearest 1 μm with an ocular micrometer (Olympus Corporation, Tokyo, Japan) attached to an inverted microscope. OCCs containing oocytes with diameters of 90–105 μm were selected.

To collect OCGCs containing fully grown oocytes, OCGCs from late antral follicles (4–6 mm in diameter) were aspirated with follicular fluid using a syringe and a needle (18 ga; Terumo Corporation, Tokyo, Japan), and the diameter of oocytes was measured. The oocytes with diameters of 115 µm or more served as the *in vivo*-fully grown control.

In vitro growth culture of OCCs

In vitro growth culture was performed as described previously (Makita *et al.*, 2016) with some modifications. Briefly, groups of 5–15 OCCs collected from at least 5 biological replicates were cultured for 14 days on Millicell inserts (cell culture inserts 0.4 µm, 30 mm diameter; Merck Millipore, Darmstadt, Germany) placed in Petri dishes (Falcon No. 351008; Becton, Dickinson and Company, Franklin Lakes, NJ, USA) at 38.5°C under a controlled humidified atmosphere of 5% O_2, 5% CO_2, and 90% N_2 for 7 days, followed by an atmosphere of 5% CO_2 in air for 7 days (Hirao *et al.*, 2012). The basic culture medium was α-minimum essential medium (αMEM, Cat. No. 11900-024; Invitrogen, Tokyo, Japan) supplemented with 5% (v/v) fetal bovine serum (FBS; ICN Biomedicals, Aurora, OH, USA), 50 µg/mL ascorbic acid 2-glucoside (Hayashibara Biochemical Laboratories, Okayama, Japan), 55 µg/mL cysteine, 0.05 µM dexamethasone, 4 mM hypoxanthine, 4% (w/v) PVP (molecular weight 360,000), 2.2 mg/mL sodium bicarbonate, and 0.08 mg/mL kanamycin sulfate (Hirao *et al.*, 2004). Based on a previous report (Makita and Miyano, 2014), the culture medium was supplemented with 10 ng/mL 17β-estradiol and 10 ng/mL androstenedione (Tokyo Chemical Industry, Tokyo, Japan). Using this medium as a control, OCCs were cultured in the medium supplemented with 1, 5, 10, and 50 mIU/mL recombinant human follicle-stimulating hormone (rhFSH; MSD KK, Tokyo, Japan). These concentrations were selected based on previous reports (Hulshof *et al.*, 1995; Cayo-Colca *et al.*, 2011). The day on which OCCs were collected was designated as day 0, and half of the culture medium was replaced with fresh medium every other day after day 4.

OCCs were examined every day for the formation of antrum-like structures by identifying visible spaces surrounded by CCs. Complexes with cytoplasmic degenerative oocytes, detachment of CCs from the zona pellucida, and collapsed complexes were classified as disintegrated complexes; all others were regarded as complexes that maintained their integrity.

After *in vitro* growth culture, the diameter of oocytes was measured as described above. Some of the oocytes were denuded mechanically, fixed with acetic acid-ethanol (1:3), and stained with 1% (w/v) aceto-orcein (FUJIFILM Wako Pure Chemical Corporation). The stages of meiotic division were assessed using Nomarski interference microscopy (Olympus Corporation). Oocytes were classified based on the morphology of chromatin and the nuclear envelope (Motlík *et al*., 1978; Hirao *et al*., 1995). The stages of oocytes before meiotic resumption were classified as filamentous chromatin (FC), stringy chromatin (SC), and germinal vesicle I–IV (GVI–IV). After resumption of meiosis, the stages were classified as early diakinesis (ED), late diakinesis (LD), metaphase I (MI), anaphase I and telophase I (AI-TI), and metaphase II (MII). Oocytes showing cytoplasmic or nuclear abnormalities were regarded as degenerated oocytes.

In vitro maturation culture of OCCs

OCCs that maintained their integrity after 14 days of *in vitro* growth culture were further used for *in vitro* maturation which was performed as described previously (Makita *et al*., 2016; Alam *et al*., 2018a) with some modifications. OCGCs collected from early and late antral follicles were also subjected to maturation and served as *in vivo* controls. Briefly, OCCs after growth culture and control OCGCs were cultured in 50 µL microdrops of maturation medium covered with paraffin oil (Kishida Chemical, Osaka, Japan) at 38.5°C under a controlled atmosphere (5% CO_2 in air) for 22 hours. Each microdrop contained 4–5 OCCs or OCGCs collected from at least 5 biological replicates. The maturation medium was medium 199 (Nissui Pharmaceutical) supplemented with 10% (v/v) FBS, 0.1 mg/mL sodium pyruvate (Nacalai Tesque, Kyoto, Japan),

2.2 mg/mL sodium bicarbonate, 0.08 mg/mL kanamycin sulfate, and 0.1 IU/mL human menopausal gonadotropin (Aska Pharmaceutical, Tokyo, Japan).

After 22 hours, oocytes were denuded mechanically using 0.1% (w/v) hyaluronidase and a narrow pipette. They were fixed with acetic acid-ethanol (1:3), and stained with 1% (w/v) aceto-orcein to assess the stage of oocyte maturation.

Preparation of histological sections

Histological sections of cultured OCCs were prepared as described previously (Alam *et al*., 2018b) with some modifications. Briefly, after *in vitro* growth culture, some of the complexes on Millicell inserts were washed once with PBS-PVA and fixed in 4% (w/v) paraformaldehyde (FUJIFILM Wako Pure Chemical Corporation) overnight. The next day, the complexes were washed three times with PBS-PVA and dehydrated using a series of increasing concentrations of ethanol (50% for 30 minutes, followed by 70%, 80%, 90%, 100% and 100% for 20 minutes each). Complexes maintaining their integrity were infiltrated and embedded in JB-4 resin (Polysciences, Warrington, PA, USA). A rotary microtome (HM 335 E; MICROM International GmbH, Walldorf, Germany) was used to make 7 µm sections from the specimens. Sections were stained with Mayer's hematoxylin solution (FUJIFILM Wako Pure Chemical Corporation) and 1% (w/v) eosin Y (FUJIFILM Wako Pure Chemical Corporation). EUKITT mounting medium (O. Kindler, Freiburg, Germany) was used to mount the sections.

Statistical analysis

Differences among mean (±SEM) diameters of oocytes were analyzed by one-way ANOVA followed by Tukey-Kramer multiple range test (Excel software with the add-in Ekuseru-Toukei 2010; Social Survey Research Information, Tokyo, Japan). All other experimental data were analyzed by a Chi-square test. Statistical significance was set at $P < 0.05$.

Results

Development of OCCs

Typical morphologies of OCCs during growth culture are shown in Figure 2A. During growth culture, the size of OCCs increased in all treatment groups. However, some of the OCCs cultured with 10 and 50 mIU/mL FSH were small, and some of them detached from the membrane sheet and floated in the medium.

The integrity of OCCs during growth culture is shown in Figure 3A. On day 7, 90% or more of OCCs maintained the structures that contained an oocyte surrounded by CCs. After day 7, the structures of some OCCs collapsed, and the oocytes were denuded. On day 14, all OCCs cultured with 1 and 5 mIU/mL FSH maintained their structures. The integrity of OCCs cultured without FSH and, with 10 and 50 mIU/mL FSH were 95%, 84%, and 78%, respectively.

OCCs formed antrum-like structures after day 5 or 6 (Fig. 3B). When FSH was added to the culture medium, OCCs formed antrum-like structures one day earlier than those cultured without FSH. On day 14, the formation rates of antrum-like structures by OCCs cultured without FSH and, with 1 and 5 mIU/mL FSH were high (93%, 93%, and 95%, respectively). In the OCCs that formed antrum-like structures, oocytes were maintained in 2–3 layers of surrounding CCs, and MGC-like cells lined the wall of the complexes (Fig. 2B, 0 and 1 mIU/mL FSH). In contrast, when OCCs were cultured with 10 and 50 mIU/mL FSH, some of the antrum-like structures collapsed during growth culture, in which all the oocytes degenerated (Fig. 2B, 50 mIU/mL FSH). Therefore, the formation rates of antrum-like structures by OCCs decreased to 79% and 63% upon treatment with 10 and 50 mIU/mL FSH, respectively, on day 14 (Fig. 3B). After growth culture, some of the OCCs that contained degenerated oocytes were sticky.

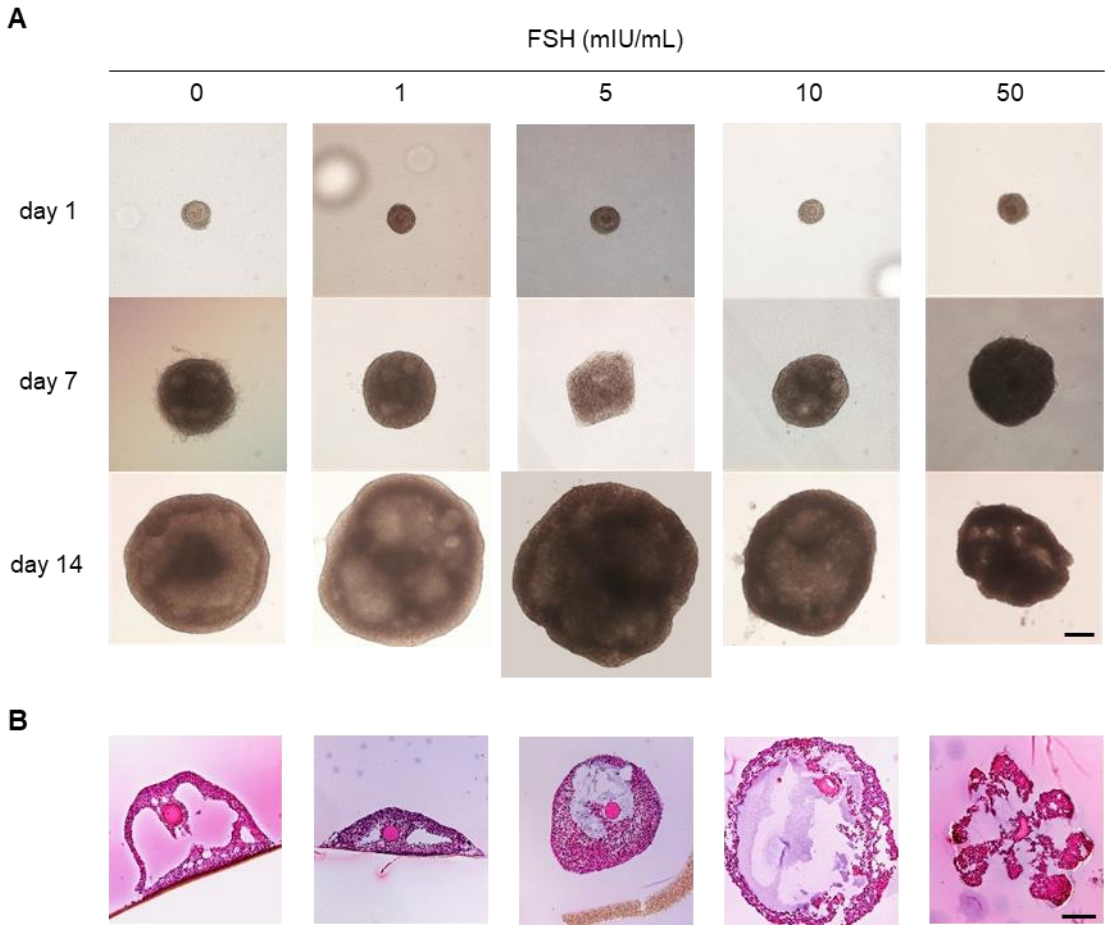

Figure 2 Typical morphologies of bovine OCCs during *in vitro* growth culture (A) and representative images of histological sections of OCCs after 14 days of culture (B). OCCs were cultured for 14 days without FSH and with varying concentrations of FSH ranging between 1–50 mIU/mL. The pictures represent OCCs on days 1, 7 and 14 (A). After OCCs attached onto a membrane sheet, they increased in size, and some of the OCCs formed antrum-like structures (A). After 14 days of culture, antrum-like structures were observed inside the complexes (B). When OCCs were cultured with 10 or 50 mIU/mL FSH, some of the antrum-like structures collapsed before the end of the culture period. OCCs cultured with higher concentrations of FSH contained degenerated oocytes. The scale bars represent 200 μm.

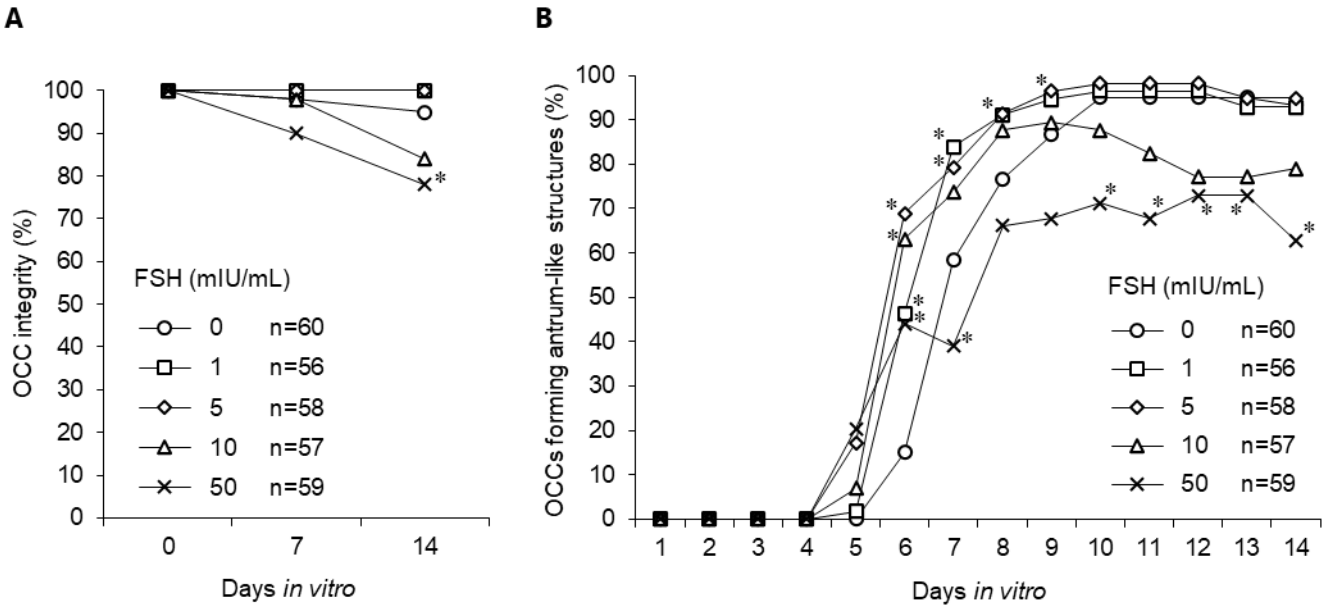

Figure 3 The integrity of bovine OCCs (A) and formation of antrum-like structures by OCCs (B) during *in vitro* growth culture. Complexes with cytoplasmic degenerative oocytes, detachment of CCs from the zona pellucida, and collapsed complexes were classified as disintegrated complexes; all others were regarded as complexes maintaining their integrity. The formation of antrum-like structures by OCCs was examined every day by identifying visible spaces surrounded by CCs. The number of complexes (n) used in each group is shown in each graph (A and B). * Values are significantly different from those of OCCs cultured without FSH (0 mIU/mL) ($P < 0.05$).

Oocyte growth in OCCs

After growth culture, the mean diameters of the oocytes in OCCs were significantly increased in all treatment groups compared to that of the oocytes before culture (Fig. 4). Oocytes cultured without FSH and with 1 mIU/mL FSH for 14 days grew to similar sizes to those of *in vivo*-fully grown oocytes collected from 4–6 mm-sized late antral follicles (122.2±0.9 μm, 118.8±1.3 μm, and 123.0±0.6 μm, respectively).

When the OCCs were cultured without FSH and with 1 mIU/mL FSH, the rates of oocytes at the GV stage were 79% and 86%, respectively, which were equivalent to or slightly lower than those of *in vivo*-fully grown oocytes (Table 1). In contrast, when the OCCs were cultured with 5–50 mIU/mL FSH, the percentages of the oocytes at GV stage were low, and the rates of degenerated oocytes increased. Some of the oocytes in OCCs cultured with 5 mIU/mL FSH degenerated even though the antrum-like structures were maintained until the end of the growth culture.

In the subsequent maturation culture experiments, 86% of the oocytes in OCCs cultured without FSH and with 1 mIU/mL FSH reached MII stage (Table 2). In contrast, the maturation rates of oocytes cultured with 5–50 mIU/mL FSH were low, and the rates of oocytes in LD, MI, and AI-TI stages and degenerated oocytes increased.

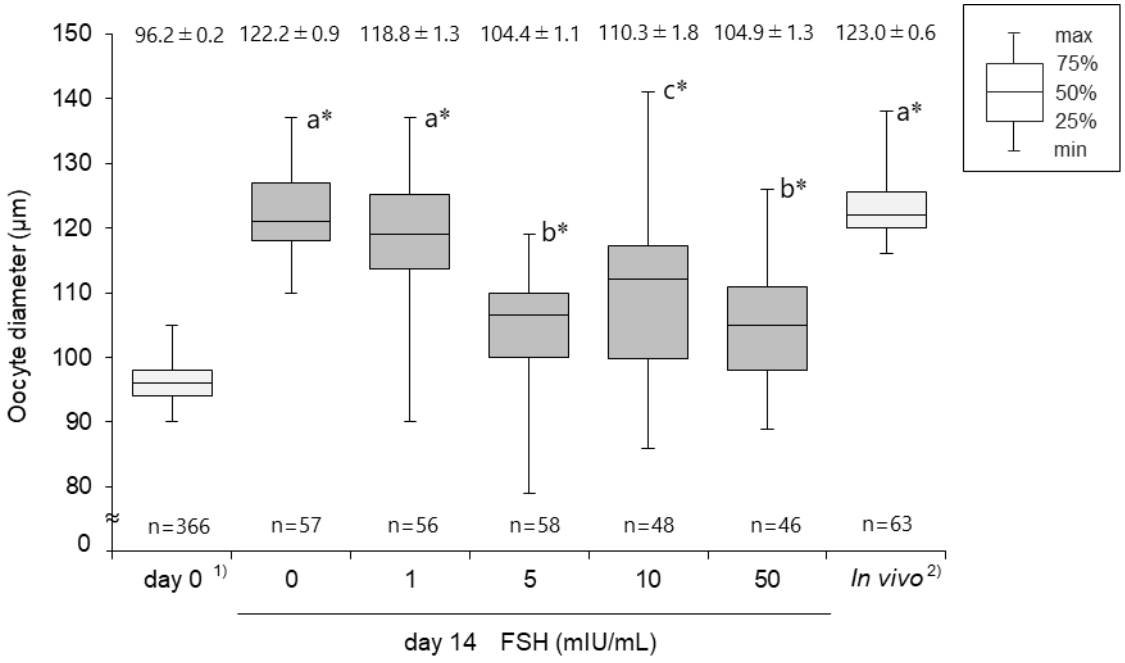

Figure 4 Diameters of bovine oocytes in OCCs after *in vitro* growth culture. The number of oocytes (n) used in each group is shown at the bottom of each box. The mean (± SEM) diameters of oocytes are shown at the top of each box. [1)] The diameter of oocytes collected from early antral follicles (0.5–0.7 mm) before culture. [2)] The diameter of fully grown oocytes collected from late antral follicles (4–6 mm). * Values are significantly different from those of oocytes before culture (day 0) ($P < 0.05$). [a-c] Different alphabets denote significantly different values ($P < 0.05$).

Table 1 Meiotic stages of *in vitro*-grown bovine oocytes in OCCs.

In vitro growth (day)	FSH (mIU/mL) [1)]	Number of oocytes used	Number (%) of oocytes at each stage [4)]																	
			FC		SC		GV		ED		LD		MI		AI – TI		MII		DG	
0 [2)]	–	48	47	(98)	1	(2)	0	(0)	0	(0)	0	(0)	0	(0)	0	(0)	0	(0)	0	(0)
14	0	29	2	(7)	2	(7)	23	(79)[a]	0	(0)	0	(0)	0	(0)	0	(0)	0	(0)	2	(7)
	1	28	1	(4)	1	(4)	24	(86)[ac]	0	(0)	2	(7)	0	(0)	0	(0)	0	(0)	0	(0)
	5	28	4	(14)	1	(4)	9	(32)[b]	6	(21)	4	(14)	0	(0)	0	(0)	0	(0)	4	(14)
	10	24	2	(8)	2	(8)	10	(42)[b]	0	(0)	1	(4)	2	(8)	0	(0)	0	(0)	7	(29)
	50	24	1	(4)	1	(4)	4	(17)[b]	2	(8)	2	(8)	0	(0)	0	(0)	0	(0)	14	(58)
In vivo [3)]	–	33	0	(0)	0	(0)	32	(97)[c]	0	(0)	1	(3)	0	(0)	0	(0)	0	(0)	0	(0)

[1)] OCCs collected from early antral follicles (0.5–0.7 mm) were cultured with varying concentrations of FSH (1–50 mIU/mL) for 14 days. [2)] Oocytes were collected from early antral follicles for culturing. [3)] Fully grown oocytes were collected from late antral follicles (4–6 mm). [4)] FC, filamentous chromatin; SC, stringy chromatin; GV, germinal vesicle I–IV; ED, early diakinesis; LD, late diakinesis; MI, metaphase I; AI-TI, anaphase I and telophase I; MII, metaphase II; DG, degeneration. [a-c] Different alphabets denote significantly different values ($P < 0.05$).

Table 2 Meiotic competence of *in vitro*-grown bovine oocytes in OCCs after *in vitro* maturation.

In vitro growth (day)	FSH (mIU/mL) [1)]	Number of oocytes used	Number (%) of oocytes at each stage [4)]															
			FC		SC		GV		ED		LD		MI		AI – TI		MII		DG	
0 [2)]	–	28	25	(89)	0	(0)	3	(11)	0	(0)	0	(0)	0	(0)	0	(0)	0	(0)	0	(0)
14	0	28	0	(0)	0	(0)	0	(0)	0	(0)	0	(0)	4	(14)	0	(0)	24	(86)[a]	0	(0)
	1	28	0	(0)	0	(0)	0	(0)	1	(3)	2	(7)	1	(3)	0	(0)	24	(86)[a]	0	(0)
	5	30	0	(0)	1	(3)	0	(0)	0	(0)	6	(20)	9	(30)	0	(0)	2	(7)[b]	12	(40)
	10	24	0	(0)	0	(0)	1	(4)	0	(0)	1	(4)	11	(46)	2	(8)	3	(13)[b]	6	(25)
	50	22	0	(0)	0	(0)	0	(0)	0	(0)	2	(9)	8	(36)	0	(0)	3	(14)[b]	9	(41)
In vivo [3)]	–	30	0	(0)	0	(0)	0	(0)	0	(0)	0	(0)	0	(0)	0	(0)	30	(100)	0	(0)

[1)] OCCs collected from early antral follicles (0.5–0.7 mm) were subjected to *in vitro* maturation culture after 14 days of *in vitro* growth culture with 1–50 mIU/mL FSH. [2)–4)] See the footnotes in Table 1. [a, b] Different alphabets denote significantly different values ($P < 0.05$).

Discussion

Irrespective of FSH supplementation to the culture medium, OCCs collected from bovine early antral follicles developed and formed antrum-like structures similar to the cultured bovine OCGCs as reported previously (Hirao *et al*., 2004, 2012; Makita and Miyano, 2014, 2015). The antrum-like structures were composed of CCs surrounding the oocyte and MGC-like cells making the complex wall. It is worth noting that CCs alone were able to form antrum-like structures, although a small number of MGCs could have been mixed in the OCCs. Antrum formation *in vivo* is accompanied by the differentiation of GCs in preantral follicles to MGCs and CCs (Diaz *et al*., 2007). Although some studies showed that OCGCs collected from early antral follicles formed antrum-like structures *in vitro* (Hirao *et al*., 2004, 2012; Makita and Miyano, 2014, 2015), it has not been clarified whether originally existing MGCs in OCGCs formed the wall of antrum-like structures, and whether CCs in OCGCs differentiated into MGC-like cells to form the wall. The present study showed that CCs in OCCs differentiate into MGC-like cells for the formation of antrum-like structures. The formation of antrum-like structures promotes oocyte growth and the acquisition of meiotic competence (Hirao *et al*., 2004; Makita and Miyano, 2014), although it is not clear whether the antrum-like structures *in vitro* have essentially the same structures as the *in vivo* antra. This structure has been thought to prevent the diffusion of growth factors and create a microenvironment for supporting oocyte growth (Hirao, 2012; Hirao *et al*., 2012).

During the culture of OCCs, there is no apparent difference in the size of OCCs among the experimental groups on day 7. After changing the oxygen concentration from 5% to 20%, the sizes of some OCCs cultured with FSH were larger than that of OCCs cultured without FSH. It is suspected that both changing the oxygen concentration and stimulation by FSH might have promoted the proliferation of CCs in OCCs. Additionally, OCCs cultured with FSH formed

antrum-like structures one day earlier than those cultured without FSH. It has been suggested that FSH is involved in the development of secondary follicles to antral follicles (Matzuk *et al*., 2002; El-Hayek *et al*., 2014; Richani and Gilchrist, 2018). When FSH was added to the medium, GCs in the preantral follicles proliferated (Hulshof *et al*., 1995), the diameter of the follicles increased (Wandji *et al*., 1996), and antrum-like structures were formed (Gutierrez *et al*., 2000; Itoh *et al*., 2002). These results show that FSH promotes antrum formation. It cannot be denied that FSH in FBS affected the formation of antrum-like structures in the present study. However, supplementation with FSH at all examined concentrations promoted formation of antrum-like structures as observed. In addition, bovine oocytes did not grow and degenerate in the absence of FBS in the present culture conditions, even when FSH was added to FBS-free medium (data not shown).

Oocytes in OCCs grew and acquired meiotic competence irrespective of the presence of FSH during growth culture. The appropriate concentration of FSH was 1 mIU/mL in the present culture system since all OCCs maintained the structures and oocytes grew fully and acquired meiotic competence at a higher rate at this concentration. In contrast, when OCCs were cultured with 10 and 50 mIU/mL FSH, some of the antrum-like structures collapsed before the end of the culture period and all the oocytes degenerated in the collapsed structures. After growth culture, some OCCs that contained degenerated oocytes were sticky. The CCs seemingly degenerated due to their exposure to high concentrations of FSH. Since CCs provide nutrients and physiologically active substances to oocytes, it is considered that the deterioration of CCs retards oocyte growth and causes degeneration of the oocytes. As all oocytes degenerated in the collapsed structures and some of the oocytes degenerated even in those that maintained structural integrity when cultured with 5 mIU/mL FSH, degeneration of oocytes might have preceded CC degeneration in OCCs. These also suggest a functional interaction between oocytes and CCs for oocyte growth was broken in the OCCs.

After 14 days of *in vitro* growth culture, 79% and 86% of the oocytes in the OCCs, that were cultured without FSH and with 1 mIU/mL FSH, respectively, were at the GV stage. During the process of oocyte growth, the nuclear stage of the oocytes reaches the GV stage from the FC and SC stages (Hirao *et al*., 1995). Therefore, oocytes cultured in OCCs progressed to the nuclear stage adequately. In addition, the mean diameters of the oocytes increased from approximately 100 μm to 120 μm, which is equivalent to the diameters of *in vivo*-fully grown oocytes. When these grown oocytes were subjected to *in vitro* maturation, more than 80% of them matured to MII. It has been demonstrated that bovine oocytes with diameters greater than 110 μm acquired meiotic competence (Fair *et al*., 1995; Hyttel *et al*., 1997). These results suggest that bovine oocytes in OCCs grow and acquire meiotic competence in the present culture system. In other words, CCs alone are able to support bovine oocyte growth *in vitro*.

In conclusion, bovine OCCs that had no MGCs formed antrum-like structures in which MGC-like cells formed the outer wall of the structures. Oocytes in the OCCs grew and acquired meiotic competence. Although FSH accelerated formation of antrum-like structures, high concentrations of FSH were not suitable for oocyte growth. These results suggest that bovine CCs are able to differentiate into MGC-like cells and fully support oocyte growth *in vitro*.

CHAPTER III

Regeneration of transzonal projections in oocyte-mural granulosa cell complexes

Introduction

In the ovary, oocytes are surrounded by GCs or CCs. GCs adhere directly to oocytes in the primordial follicles. As the follicles develop, the surrounding GCs alter their morphology from squamous to cuboidal shape, and the zona pellucida is formed around the oocytes. GCs extend TZPs penetrating the zona pellucida to maintain contact with the oocytes. After antrum formation, GCs differentiate into CCs and MGCs. CCs surrounding the oocyte maintain contact with the oocyte *via* TZPs, while MGCs apart from the oocyte proliferate lining the basement membrane of the antral follicle.

Bidirectional communication between oocytes and GCs regulates both types of cells throughout the follicular developmental stages (Eppig, 2001; Matzuk *et al*., 2002). This communication is thought to be mediated through paracrine signaling and gap junctional communication at the ends of TZPs (Matzuk *et al*., 2002; Veitch *et al*., 2004; Teilmann, 2005; Clarke, 2018a, 2018b). Oocyte-derived growth factors regulate GC development and function, and nutrients and mRNA from GCs or CCs are transported through TZPs for oocyte growth (Eppig *et al*., 2005; Su *et al*., 2008, 2009; Macaulay *et al*., 2014, 2016). Studies of *in vitro* growth culture of mammalian oocytes have used oocyte-somatic cell complexes or whole follicles (Hirao, 2011) because somatic cells—especially GCs and CCs—surrounding oocytes are essential for oocyte growth (Clarke, 2018a, 2018b, 2022). TZPs are important structures for the successful growth of oocytes *in vitro*.

Barrett *et al*. (2010) showed that the number of TZPs, which had decreased by

cryopreservation, increased during subsequent *in vitro* growth culture of mouse, monkey, and human secondary follicles, and suggested that interactions between GCs and oocytes were regenerated. Recently, El-Hayek *et al.* (2018) reported that mouse GCs developed new TZPs in reconstructed OGCs. In livestock animals, Oi *et al.* (2015) demonstrated that porcine DOs cultured in reconstructed OGCs grew and acquired the ability to develop into blastocysts. These studies suggest that GCs regenerate TZPs. In Chapter II, bovine CCs changed to MGC-like cells in cultured OCCs as they developed antrum-like structures. Reversely, do MGCs from antral follicles regenerate TZPs as GCs and CCs do?

In this chapter, I confirmed the disappearance of TZPs by denudation of bovine growing oocytes. Then, I examined the regeneration of TZPs during the coculture of TZP-free DOs with MGCs. As the cytoskeletons of TZPs are primarily composed of F-actin (Albertini *et al.*, 2001; Barrett *et al.*, 2010; Li and Albertini, 2013; Macaulay *et al.*, 2014, 2016; El-Hayek *et al.*, 2018), regeneration of TZPs was examined by detecting F-actin with phalloidin staining. Additionally, effects of FSH on the reconstruction of complexes and the regeneration of TZPs were also examined.

Materials and methods

Chemicals

All chemicals were purchased from Sigma-Aldrich unless otherwise stated.

Collection of DOs and MGCs

OCGCs were collected from bovine early antral follicles as described in Chapter II. OCGCs were used to prepare DOs and MGCs. First, OCCs and MGCs were separated from OCGCs as described in Chapter II. Subsequently, CCs were removed completely from the OCCs using a narrow pipette and DOs were collected. The diameter of DOs (excluding the zona pellucida) was measured to the nearest 1 μm with an ocular micrometer attached to an inverted microscope. Oocytes with diameters 90–105 μm were selected for further analysis.

To collect fully grown oocytes, OCGCs from late antral follicles (4–6 mm in diameter) were aspirated with follicular fluid using a syringe and a needle (18 ga; Terumo Corporation). From the OCGCs, CCs and MGCs were removed completely using a narrow pipette, and then the diameter of the collected DOs was measured. The DOs with diameters of 115 μm or more served as the *in vivo*-fully grown control.

Preparation of TZP-free DOs and coculture with MGCs

TZP-free oocytes were prepared from DOs collected from early antral follicles. Groups of 2–10 DOs collected from at least 4 biological replicates were cultured individually in 12 μL microdrops of culture medium covered with paraffin oil in Petri dishes (Falcon No. 351007; Becton, Dickinson and Company) at 38.5°C under a controlled humidified atmosphere of 5% O_2, 5% CO_2, and 90% N_2 for 24 hours. The culture medium was the basic culture medium supplemented with 10 ng/mL 17β-estradiol and 10 ng/mL androstenedione as described in

Chapter II. DOs were cultured in the medium supplemented with or without 1 mIU/mL rhFSH. This concentration was selected based on the results in Chapter II. The disappearance of TZPs was assessed after culturing for 24 hours.

To reconstruct oocyte-mural granulosa cell complexes, the masses of MGCs with a size larger than that of the DOs were collected from early antral follicles. The collected MGCs were cocultured with TZP-free DOs individually in 12 μL microdrops of culture medium in Petri dishes (Falcon No. 351007). After coculture for 24 hours, the reconstructed complexes in which MGCs adhered to DOs (DO+MGCs), were transferred to Millicell inserts (cell culture inserts 0.4 μm, 30 mm diameter; Merck Millipore) placed in Petri dishes (Falcon No. 351008). The regeneration of TZPs was examined after coculture for 24, 48, 72, 96, and 120 hours.

Fluorescence microscopy

To identify the TZPs rich in actin filaments, fluorescence microscopy was performed as described previously (Makita and Miyano, 2014) with some modifications. Briefly, the oocytes surrounded by CCs or MGCs were denuded mechanically. The denuded oocytes were washed twice in PBS-PVA and fixed in 4% paraformaldehyde in PBS-PVA for 60 minutes. After being washed twice in PBS-PVA, the fixed oocytes were stored in PBS-PVA containing 1 mg/mL bovine serum albumin (BSA) (PBS-PVA-BSA) at 4°C overnight. The oocytes were then incubated with Alexa Fluor 488 conjugated phalloidin (8.25 nM in PBS-PVA-BSA; A12379; Molecular Probes, Invitrogen, Carlsbad, CA, USA) at 38.5°C under controlled atmosphere (5% CO_2 in air) for 90 minutes. They were then washed three times for 15 minutes each in PBS-PVA-BSA and mounted on glass slides with ProLong Gold antifade reagent with DAPI (P36931; Molecular Probes). The TZPs were visualized under a confocal laser scanning microscope (FV1000-KDM; Olympus Corporation). The number of visible actin-based TZPs that penetrated the zona pellucida to reach the oocyte surface was counted in the widest cross-section of the oocytes.

Statistical analysis

The number of TZPs was analyzed by one-way ANOVA followed by the Tukey-Kramer multiple range test (Excel software with the add-in Ekuseru-Toukei 2010). The number of TZPs was also analyzed using Smirnov-Grubbs' outlier test ($P < 0.05$). Statistical significance was set at $P < 0.05$.

Results

Reconstruction of DO+MGC complexes

Typical morphologies of DO+MGCs during culture are shown in Figure 5. Oocytes collected from early antral follicles were denuded (Fig. 5, a0, b0), and 24 hours after denudation, the DOs were cocultured with the mass of MGCs in new microdrops (Fig. 5, a1, b1). After coculture for 24 hours, the MGCs adhered to the DOs and the culture substrate (Fig. 5, a2, b2). All the DOs that had been kept on the mass of MGCs for 24 hours after starting coculture became surrounded by MGCs, and complexes (DO+MGCs) were reconstructed. When the DOs tumbled down and were away from the MGCs during the coculture, the MGCs did not adhere to the DOs and the complex did not form. DO+MGCs were picked up with a pipette and transferred onto Millicell inserts (Fig. 5, a2', b2'). After coculture for 48 hours, the DO+MGCs attached onto a membrane sheet (Fig. 5, a3, b3) and constructed spherical structures. The size of the DO+MGCs cultured without FSH increased gradually (Fig. 5, a3–6) similar to complexes cultured with 1 mIU/mL FSH (Fig. 5, b3–6).

Disappearance and regeneration of TZPs

TZPs were observed throughout the zona pellucida of growing and fully grown oocytes, and some of the TZPs penetrated the zona pellucida to reach the oocyte surface (Fig. 6, a, b). In the oocytes collected from early and late antral follicles, the mean number of TZPs that reached the oocyte surface was 100.4±3.8 and 98.7±3.6, respectively (Fig. 7).

The mean number of TZPs decreased in oocytes cultured with or without FSH (2.6±0.9 and 1.8±0.5, respectively) 24 hours after denudation (Fig. 6, c1, d1; Fig. 7). When DO+MGCs were cultured without FSH, the number of TZPs increased gradually during coculture, and after 72–120 hours in some oocytes, it reached a similar number to that in the oocytes *in vivo* (Fig. 7).

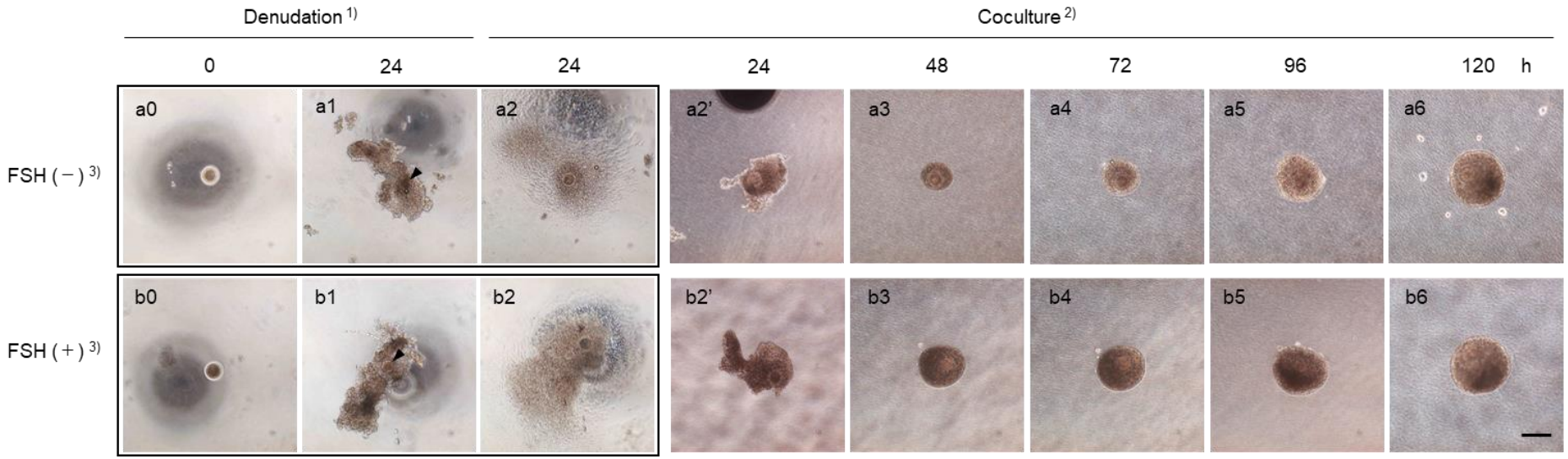

Figure 5 Typical morphologies of bovine DOs, and DO and MGCs (DO+MGCs) during coculture up to 120 hours. DOs collected from early antral follicles (0.5–0.7 mm) cultured in microdrops of culture medium (a0, b0). DOs cocultured with MGCs 24 hours after denudation (day 1) (a1, b1). After coculture for 24 hours (a2, b2), DO+MGCs were transferred to Millicell inserts (a2', b2') and cultured until 120 hours (a3–6, b3–6). The images framed in black indicate DOs and DO+MGCs cultured in microdrops. The arrowheads indicate DOs. The scale barrepresents 200 µm. [1)] DOs collected from early antral follicles were cultured for 24 hours. [2)] DOs cultured with MGCs 24 hours after denudation, for up to 120 hours. [3)] DOs and DO+MGCs were cultured without FSH (FSH (−)) or with 1 mIU/mL FSH (FSH (+)).

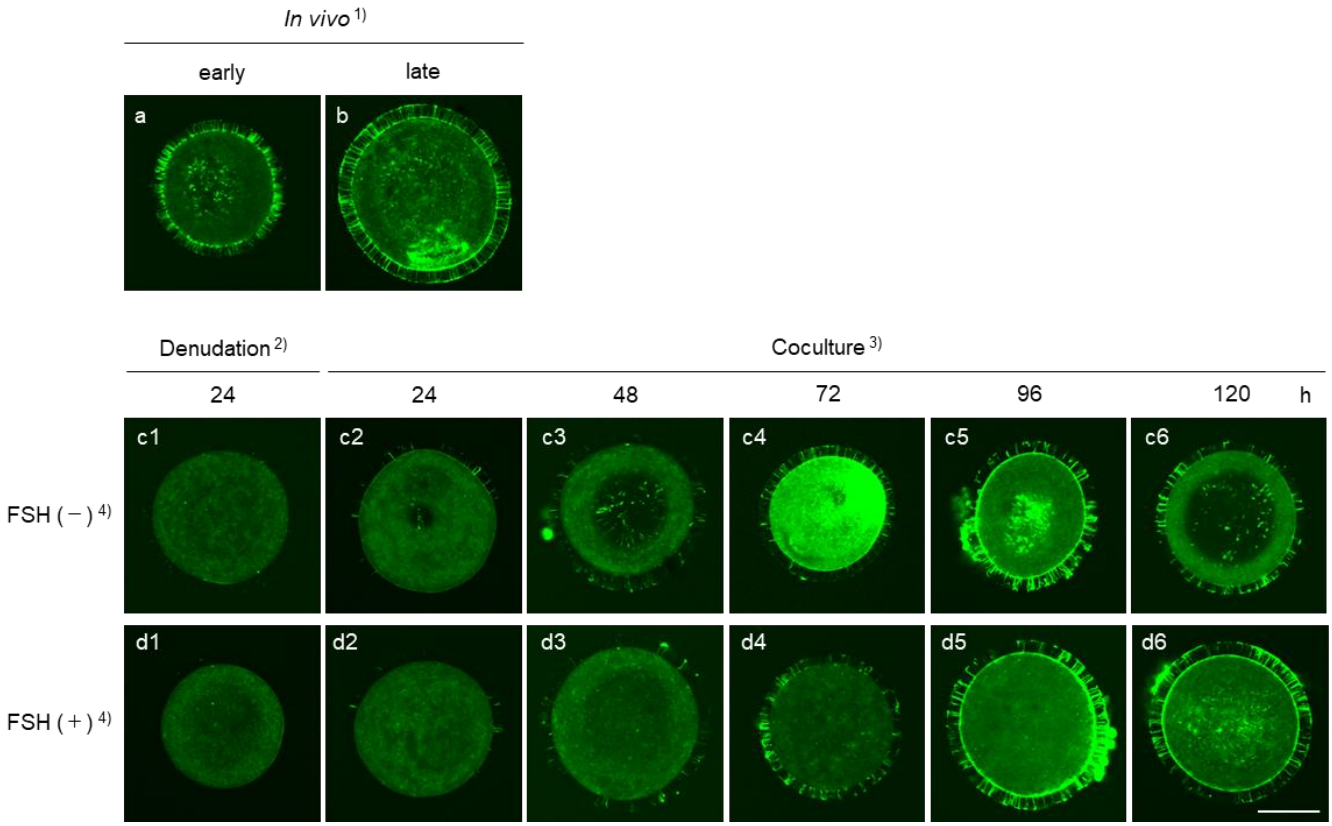

Figure 6 Fluorescent staining of oocytes showing TZPs in bovine oocytes after denudation and coculture with MGCs. TZPs were observed throughout the zona pellucida of oocytes collected from early antral follicles (a) and late antral follicles (b), and some TZPs penetrated the zona pellucida to reach the oocyte surface. The disappearance of TZPs 24 hours after denudation (c1, d1). Gradual regeneration of TZPs after coculture of DOs with MGCs (c2–6, d2–6). Alexa Fluor 488 conjugated phalloidin stained F-actin green. The scale bar represents 50 μm. [1)] *In vivo*-growing oocytes collected from early antral follicles (0.5–0.7 mm) and fully grown oocytes collected from late antral follicles (4–6 mm). [2)] DOs collected from early antral follicles were cultured for 24 hours. [3)] DOs cocultured with MGCs 24 hours after denudation, for 24–120 hours. [4)] DOs and DO+MGCs were cultured without FSH (FSH (−)) or with 1 mIU/mL FSH (FSH (+)).

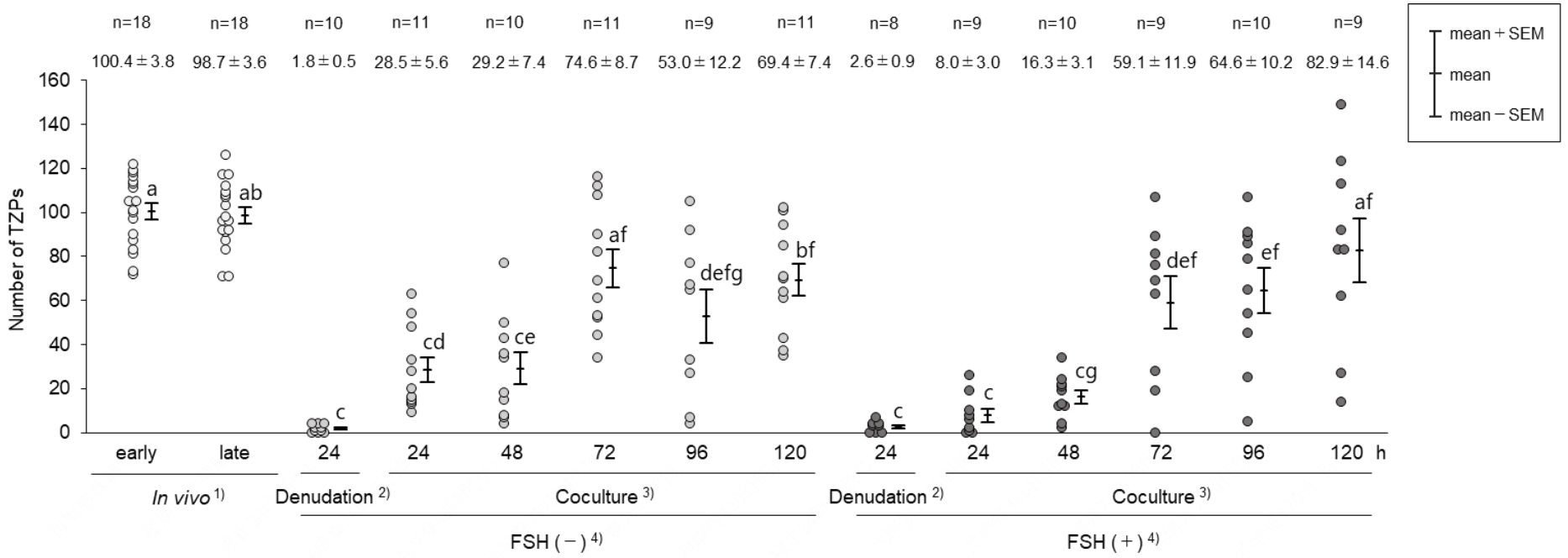

Figure 7 Changes in the number of TZPs in bovine oocytes after denudation and coculture with MGCs. The number of visible actin-based TZPs that penetrated the zona pellucida to reach the oocyte surface was counted in the widest cross-section of the oocytes. The number of oocytes (n) used in each group and the mean (± SEM) number of TZPs are shown at the top. [1)–4)] See the legend of Figure 6. [a–g] Different letters denote significantly different values ($P < 0.05$).

In contrast, when DO+MGCs were cultured with FSH, the mean numbers of TZPs 24–48 hours after coculture with MGCs were fewer than that in oocytes cultured without FSH, although the difference was not significant. However, 72–120 hours after coculture, the number of TZPs in some oocytes was similar to that in the oocytes *in vivo*.

Discussion

Denudation of bovine oocytes induced the disappearance of TZPs. Since actin-based TZPs extend from GCs or CCs to the oocyte (Albertini *et al*., 2001; Barrett *et al*., 2010; Li and Albertini, 2013; Macaulay *et al*., 2014, 2016; El-Hayek *et al*., 2018), the mechanical disconnection of TZPs from CCs by pipetting seems to induce actin depolymerization in the TZPs. In the present experiment, almost all TZPs disappeared 24 hours after denudation. Therefore, the DOs cultured for 24 hours are considered to be TZP-free DOs.

Irrespective of the presence of FSH in the culture medium, the coculture of TZP-free DOs with MGCs caused MGCs to adhere to TZP-free DOs to reconstruct complexes. MGCs surrounded DOs in a manner similar to CCs, and the resulting DO+MGCs developed into spherical structures. Within the structures, TZPs were regenerated. The newly generated TZPs extended from MGCs and penetrated the zona pellucida to reach the oocyte surface. Since the defect of zona pellucida affects the morphology of TZPs and apoptosis of GCs (Wang *et al*., 2019), the integrity of zona pellucida is thought to be maintained after oocyte denudation for regeneration of TZPs in this culture system.

After coculture, the number of TZPs increased with the development of DO+MGCs. The number of TZPs in some oocytes after coculture for 72 hours without FSH became similar to that in *in vivo* oocytes, suggesting that MGCs first surround the oocytes and elaborate TZPs toward the oocytes. Mizumachi *et al*. (2018) have suggested that the culture medium viscosity is involved in strengthening the contact between oocytes and CCs. Therefore, the addition of PVP to the present culture media may have supported the maintenance of the complex while preventing MGC migration and preserving cell adhesion as TZPs developed.

When DO+MGCs were cultured with FSH, the mean numbers of TZPs 24–48 hours after coculture with MGCs were fewer than that in oocytes cultured without FSH. This result

suggests that FSH retarded regeneration of TZPs by MGCs. In mice carrying a targeted deletion of the *FSHβ* subunit gene, TZP density increased; in contrast, FSH treatment resulted in a retraction of TZPs (Combelles *et al.*, 2004). Some studies have reported a negative effect of FSH on gap junctions between bovine CCs and oocytes, and suggest that a dose of FSH induces a retraction of TZPs (McLaughlin *et al.*, 2010; Luciano *et al.*, 2011; Buratini *et al.*, 2022). Based on these considerations, in the present study, FSH seems to have a negative effect on TZP regeneration in reconstructed complexes, although it has a positive effect on the antrum formation by OCCs shown in the previous chapter.

It has been suggested that opposing gradients of FSH and oocyte-derived factors in mouse antral follicles cause the different expression of transcript subsets in MGCs and CCs (Diaz *et al.*, 2007). The present study showed that MGCs collected from early antral follicles have the ability to develop TZPs similar to CCs in antral follicles. Some reports suggest that growth differentiation factor 9 (GDF9) produced by oocytes is involved in the formation and extension of TZPs in mice (Carabatsos *et al.*, 1998; El-Hayek *et al.*, 2018). El-Hayek *et al.* (2018) have suggested that GDF9 controls the mRNA levels of the general components of filopodia (*Daam1*, dishevelled associated activator of morphogenesis 1; *Fscn1*, fascin actin-bundling protein 1; *Myo10*, myosin heavy chain 10) in CCs, and that GDF9 probably affects the number of TZPs. Baena and Terasaki (2019) have proposed that GCs search for oocytes through their cytoplasmic projections. In their proposed model, a contact-mediated paracrine interaction with the oocyte induces GCs to exhibit a CC-specific phenotype and the contacting projections become TZPs. Although the control mechanism of TZP extension has not been well elucidated, I speculate that MGCs that adhered to DOs in the present experiment received oocyte-derived factors, regenerated and extended TZPs, and became CC-like cells.

In conclusion, the results in this chapter suggest that MGCs collected from bovine early antral follicles are able to reconstruct complexes with TZP-free DOs and regenerate TZPs, that is

to say, the MGCs become CC-like cells. Additionally, it is thought that FSH has a negative effect on the regeneration of TZPs by the MGCs in the present experimental system.

CHAPTER IV

Change in the ability of granulosa cells to extend transzonal projections during follicle development

Introduction

As secondary follicles develop and form antra, GCs differentiate into CCs surrounding oocytes and MGCs lining the follicle wall (Matzuk *et al*., 2002; Hummitzsch *et al*., 2015). These two types of cells have different phenotypes and different roles in the follicle (Hummitzsch *et al*., 2015; Juengel and McNatty, 2005). MGCs have a role in estrogen synthesis and control the estrous cycle. In contrast, CCs keep direct connections with oocytes through TZPs and support oocyte growth. Although MGCs do not contact oocytes, they also support oocyte growth indirectly in paracrine manners (Zhang *et al*., 2010; Conti *et al*., 2012; Clarke, 2018b). MGCs produce natriuretic peptide precursor type C (NPPC) which stimulates NPPC receptor (NPR2) in CCs, and CCs increase cyclic guanosine monophosphate (cGMP) levels. cGMP is transported to oocytes through TZPs, and maintains meiotic arrest of oocytes (Richard and Baltz, 2014; Clarke, 2018b). As the antrum develops, growing oocytes acquire the ability to resume meiosis (Fair *et al*., 1995; Hyttel *et al*., 1997; Tsuji *et al*., 2012). CCs and MGCs cooperatively prevent a precocious meiotic resumption of growing oocytes (Russell and Robker, 2007; Jaffe and Egbert, 2017; Alam and Miyano, 2019; Dass and Arur, 2022). Although MGCs and CCs have different roles, these two types of cells cooperate for growth and meiotic arrest of oocytes in antral follicles.

It has been considered that the default pathway of GC differentiation proceeds to the MGC phenotype (Eppig *et al*., 1997), and oocyte-derived factors, such as GDF9 and bone morphogenetic protein 15 (BMP15), promote GC differentiation into the CC phenotype (Eppig, 2001; Juengel and McNatty, 2005). In mice, some studies have reported that MGCs and CCs

express different subsets of transcripts in antral follicles (Diaz *et al*., 2007; Wigglesworth *et al*., 2015), and suggested that oocytes control several gene expressions in CCs (Sugiura *et al*., 2005; Emori *et al*., 2020). It is supposed that a concentration gradient of oocyte-derived factors in the antral follicles causes these two different cell types to play different roles. Then, why were the bovine CCs collected from early antral follicles able to make antrum-like structures containing MGC-like cells in Chapter II? Additionally, why were the MGCs collected from early antral follicles able to regenerate TZPs and support oocyte growth like CCs in Chapter III? Furthermore, it has not been clear the relation between the ability of GCs to extend TZPs and the transcriptome change from GCs to MGCs.

In Chapter III, MGCs collected from early antral follicles adhered to DOs to reconstruct complexes, following which, TZPs were regenerated over time. Using this method, in this chapter, I examined whether GCs from secondary follicles and MGCs from late antral follicles were able to reconstruct complexes with DOs and regenerate TZPs similar to MGCs from early antral follicles. Furthermore, to confirm that the regenerated TZPs were functional, the integrity of reconstructed complexes and antrum formation were examined throughout the subsequent growth culture period. After culture, the number of TZPs, the diameters of oocytes, and the meiotic competence of oocytes were determined. Then, the transcriptome was analyzed among GCs, CCs, and MGCs collected from three different sized follicles.

Materials and methods

Chemicals

All chemicals were purchased from Sigma-Aldrich unless otherwise stated.

Collection of DOs, GCs, and MGCs

OGCs were collected from bovine secondary follicles (0.2–0.4 mm in diameter) to prepare GCs. Oocytes were removed from the OGCs using a narrow pipette and the GCs were collected. OCGCs were collected from early antral follicles (0.5–0.7 mm in diameter) as described in Chapter II. From the OCGCs, DOs and MGCs were collected as described in Chapter III. MGCs were collected also from late antral follicles (4–6 mm in diameter). The diameter of oocytes in OCGCs and DOs (excluding the zona pellucida) from early antral follicles was measured to the nearest 1 μm with an ocular micrometer attached to an inverted microscope. Oocytes with diameters 90–105 μm were selected for further analysis.

OCGCs containing fully grown oocytes were collected from late antral follicles as described in Chapter II, and DOs were collected as described in Chapter III. The oocytes with diameters of 115 μm or more served as the *in vivo*-fully grown control.

Reconstruction of DO+GC/MGC complexes

To prepare TZP-free DOs, groups of 4–14 DOs collected from early antral follicles from at least 3 biological replicates were cultured individually in 12 μL microdrops of culture medium for 24 hours as described in Chapter III. The culture medium was the basic culture medium supplemented with 10 ng/mL 17β-estradiol and 10 ng/mL androstenedione as described in Chapter II. Since it was found that FSH delayed the regeneration of TZPs in Chapter III, the culture medium without FSH was used in this chapter.

To reconstruct oocyte-granulosa cell complexes and oocyte-mural granulosa cell complexes, 2–3 masses of GCs from secondary follicles, and masses of MGCs, with a size larger than that of the DOs, from early and late antral follicles were prepared as described above. Collected GCs and MGCs were cocultured with TZP-free DOs individually in 12 μL microdrops of the culture medium for 24 hours. After coculture, the reconstructed complexes in which GCs and MGCs adhered to DOs (DO+GCs and DO+MGCs) were transferred to Millicell inserts (cell culture inserts 0.4 μm, 30 mm diameter; Merck Millipore) placed in Petri dishes (Falcon No. 351008) and cultured for 4 or 12 days. The reconstructed complexes were cultured at 38.5℃ under a controlled humidified atmosphere of 5% O_2, 5% CO_2, and 90% N_2 for 5 days, followed by an atmosphere of 5% CO_2 in air for 7 days (Hirao *et al.*, 2012). The day on which DOs were collected was designated as day 0, and half of the culture medium was replaced with fresh medium every other day after day 6.

The regeneration of TZPs was examined on day 6 and day 14. To identify the TZPs rich in actin filaments, fluorescence microscopy was performed as described in Chapter III.

In vitro growth culture of complexes

In vitro growth culture of DO+GCs and DO+MGCs (after 24 hours of denudation and 24 hours of reconstruction) was performed on Millicell inserts as described above for 12 days (total 14 days). As the control, groups of 9–14 OCGCs collected from early antral follicles from at least 7 biological replicates were cultured for 14 days on Millicell inserts placed in Petri dishes (Falcon No. 351008) in the same condition; at 38.5℃ under a controlled humidified atmosphere of 5% O_2, 5% CO_2, and 90% N_2 for 7 days, followed by an atmosphere of 5% CO_2 in air for 7 days. The formation of antrum-like structures by the complexes was examined daily by identifying visible spaces surrounded by somatic cells. Complexes with cytoplasmic degenerative oocytes, detachment of somatic cells from the zona pellucida, and collapsed complexes were

classified as disintegrated complexes; all others were regarded as complexes that maintained their integrity.

After culture, the diameter of the oocytes was measured as described above. Some of the oocytes were denuded mechanically to examine the meiotic stages. The meiotic stages were assessed as described in Chapter II. Oocytes showing cytoplasmic or nuclear abnormalities were regarded as degenerated oocytes. The meiotic stages of oocytes collected from late antral follicles were also examined and served as *in vivo* controls.

In vitro maturation culture of complexes

The DO+GCs, DO+MGCs, and OCGCs that maintained their integrity after *in vitro* growth culture were further used for *in vitro* maturation, which was performed as described in Chapter II. OCGCs collected from early and late antral follicles were also subjected to maturation and served as *in vivo* controls. Each microdrop contained 3–5 complexes collected from at least 4 biological replicates.

After 22 hours, the oocytes were denuded mechanically using 0.1% (w/v) hyaluronidase and a narrow pipette. They were then fixed and stained to assess the stage of oocyte maturation as described in Chapter II.

RNA sequencing analysis

To perform RNA sequencing (RNA-seq) analysis of GCs collected from secondary follicles, and CCs and MGCs collected from early and late antral follicles, RNA-seq libraries were constructed. To prepare CCs, OCCs were collected from early and late antral follicles as described in Chapter II. Oocytes were removed from the OCCs using a narrow pipette and the CCs were collected. Total RNA extraction, first-strand cDNA synthesis, cDNA amplification, and generation of sequencing libraries were performed with 1/2 volumes of the SMART-Seq v4 Ultra

Low Input RNA Kit (Takara Bio USA, San Jose, CA, USA) and the Nextera XT DNA Library Preparation Kit (Illumina, San Diego, CA, USA) according to the manufacturers' protocols. Twelve cycles of PCR were applied to the library DNA. After PCR, the library DNA was purified using the SPRIselect (Beckman Coulter, Brea, CA, USA) instead of AMPure XP beads (Beckman Coulter). Sequencing of the libraries was performed with HiSeq X (Illumina). Four GCs collected from secondary follicles, five CCs and five MGCs collected from early and late antral follicles were sequenced.

Sequence data analysis

RNA-seq reads were processed prior to analysis as described previously (Mishina *et al.*, 2021) with some modifications. Hisat2 (v2.1.0) (Kim *et al.*, 2015) with '-p 16 -x' options was used to map the reads to the ARS-UCD1.2.105 genome assembly of the bovine genome after trimming adaptor sequences and low-quality bases using fastp (v0.20.0) (Chen *et al.*, 2018) with '-w 16 --trim-poly-x --detect_adapter_for_pe_h' options. The resulting binary alignment/map (BAM) files were sorted using samtools (v1.10) (Li *et al.*, 2009). The featureCounts (v2.0.0) (Liao *et al.*, 2014) tool of Subread package with '-T 16 -F GTF -t exon -g gene_id -p -o' options was used to generate counts of reads multi-mapped to annotated genes using the gene annotation for *Bos taurus* (Ensembl, ARS-UCD1.2.105).

Based on the $\log_{10}$ transformed transcripts per kilobase million (TPM) values of the expression, principal component analysis (PCA) was conducted using R (https://www.r-project.org/) , *t*-distributed stochastic neighbor embedding (*t*-SNE) plots were visualized using Rtsne package (v0.16) (Krijthe, 2015), and marker genes for cluster were searched using MGFR package (v1.22.0) (Amrani *et al.*, 2019) in R.

Differentially expressed genes (DEGs) (false discovery rate, FDR $<$ 0.05) were identified with edgeR package (v3.38.1) (Robinson *et al.*, 2010) in R, which normalizes library

sizes with the trimmed mean of M values (TMM) method, using the dataset of the gene expressed in at least one sample. Gene ontology (GO) analysis using DEGs was performed using DAVID Cellular Component (v2022q3) (https://david.ncifcrf.gov/) (Huang *et al*., 2007).

Statistical analysis

The differences between mean (±SEM) diameters of *in vitro*- and *in vivo*-grown oocytes, and the mean number of TZPs were analyzed by one-way ANOVA followed by the Tukey-Kramer multiple range test (Excel software with the add-in Ekuseru-Toukei 2010). The number of TZPs was also analyzed using Smirnov-Grubbs' outlier test ($P < 0.05$). All other experimental data were analyzed by the Chi-square test. Statistical significance was set at $P < 0.05$.

Results

Reconstruction of DO+GC/MGC complexes and regeneration of TZPs

TZP-free DOs were cultured with GCs and two kinds of MGCs for 6 days to examine the reconstruction of complexes. Typical morphologies of DO+GCs and DO+MGCs during growth culture are shown in Figure 8. Oocytes collected from early antral follicles were denuded (Fig. 8, a0, b0, c0), and 24 hours after denudation, the DOs were cocultured with 2–3 masses of GCs from secondary follicles (referred to as "GCs") (Fig. 8, a1), and masses of MGCs from early and late antral follicles (referred to as "early MGCs" and "late MGCs", respectively) in new microdrops (Fig. 8, b1, c1). After coculture for 24 hours, GCs and early MGCs adhered to the DOs and the culture substrate (Fig. 8, a2, b2). All the DOs that had been kept on masses of GCs and early MGCs for 24 hours after starting coculture were surrounded by GCs and MGCs, and complexes (DO+GCs and DO+early MGCs) were reconstructed. The reconstructed complexes were picked up with a pipette and transferred onto Millicell inserts (Fig. 8, a2', b2'). After culture, the reconstructed complexes attached onto membrane sheets and developed as spherical structures (Fig. 8, a3, b3). In contrast, after coculture for 24 hours, most of the late MGCs barely adhered to the DOs and the culture substrate (Fig. 8, c2). The complexes in which late MGCs partially adhere to the DOs were picked up and transferred onto Millicell inserts (Fig. 8, c2'). After transferring onto Millicell inserts, these complexes did not attach to the membrane sheets. Late MGCs aggregated solidly and some of the oocytes were pushed out of the complexes during culture (Fig. 8, c3). On day 6, although some late MGCs contained the oocytes (39%), it was hard to denude the oocytes from these complexes mechanically using a narrow pipette. Thus, almost denuded oocytes (61%) were used to examine the regeneration of TZPs.

On day 6, regenerated TZPs were observed in oocytes cocultured with GCs and early MGCs (Fig. 9, a1, b1), and the number of TZPs increased compared to oocytes 24 hours after

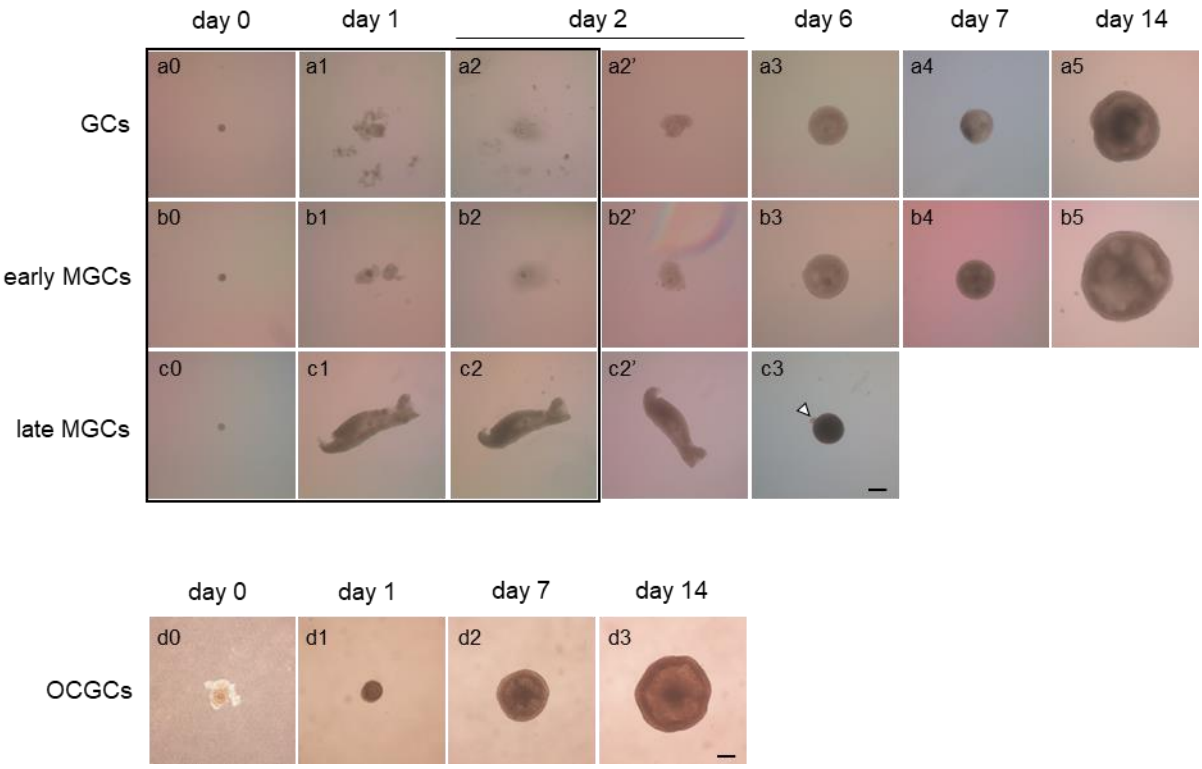

Figure 8 Typical morphologies of bovine DO+GC/MGC complexes and OCGCs during *in vitro* growth culture. DOs collected from early antral follicles (0.5–0.7 mm) cultured in microdrops of culture medium (a0, b0, c0). DOs cocultured with GCs (a1), early MGCs (b1), and late MGCs (c1) 24 hours after denudation (day 1). After coculture for 24 hours, DO+GCs (a2) and DO+MGCs (b2, c2) were transferred to Millicell inserts (a2', b2', c2') and continued culture (a3–5, b3–5, c3). On day 6, late MGCs aggregated solidly and some of the oocytes were pushed out of the complexes during culture (c3). The arrowhead indicates a pushed-out oocyte. The images framed in black indicate DOs, DO+GCs, and DO+MGCs cultured in microdrops. As the control, OCGCs collected from early antral follicles were cultured for 14 days on Millicell inserts (d0–3). The scale bars represent 200 μm.

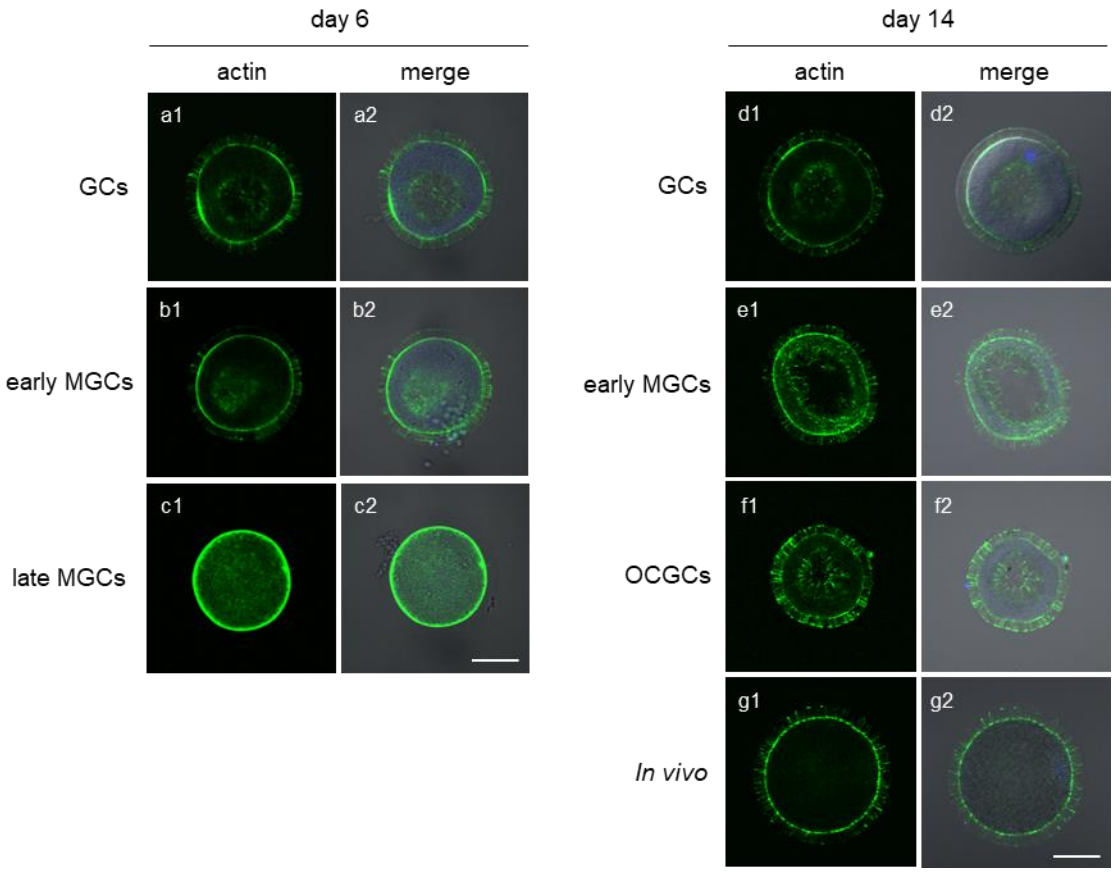

Figure 9 Fluorescent staining of bovine oocytes showing TZPs in reconstructed complexes during *in vitro* growth culture. On day 6, regenerated TZPs were observed in oocytes cocultured with GCs (a1) and early MGCs (b1). However, regenerated TZPs were hardly observed in oocytes cocultured with late MGCs (c1). On day 14, many TZPs in reconstructed complexes (d1, e1) penetrated the zona pellucida to reach the oocyte surface in a manner similar to the TZPs in OCGCs (f1) and *in vivo*-fully grown oocytes (g1). Alexa Fluor 488 conjugated phalloidin stained F-actin green (a1–g1), and DAPI stained chromatin blue. Bright field images are merged with fluorescent staining images (a2–g2). The nucleus is often not observed in the widest cross-section of oocytes due to being out of focus. The scale bars represent 50 μm.

denudation (Fig. 10). However, regenerated TZPs were hardly observed in oocytes cocultured with late MGCs (Fig. 9, c1; Fig. 10). Therefore, this experimental group was excluded from further analyses.

Development of reconstructed complexes and oocyte growth

Continuing the growth culture until day 14, the reconstructed complexes with GCs (Fig. 8, a4, 5) and early MGCs (Fig. 8, b4, 5) grew similarly to the control OCGCs (Fig. 8, d2, 3). The integrity of reconstructed complexes and OCGCs during culture is shown in Figure 11A. On day 2, 96% of the DOs were surrounded by GCs, and all the DOs were surrounded by early MGCs. Because some of the DOs had been away from and were not surrounded by GCs and early MGCs during coculture, the integrity of reconstructed complexes decreased. On day 7, 93% of the reconstructed complexes and 99% of the OCGCs maintained the structures. However, as the coculture progressed, some of the structures of reconstructed complexes and OCGCs collapsed, and the oocytes became denuded. On day 14, OCGCs showed higher integrity than DO+GCs and DO+early MGCs (94%, 88%, and 90%, respectively).

As the complexes developed, some formed antrum-like structures (Fig. 8, a3–5, b3–5, d2, 3). OCGCs started forming antrum-like structures on day 4, that was one or two days earlier than the reconstructed complexes (Fig. 11B). On day 14, OCGCs showed higher formation rates of antrum-like structures than DO+GCs and DO+early MGCs (90%, 76%, and 77%, respectively).

After 14 days of growth culture, many TZPs in reconstructed complexes penetrated the zona pellucida to reach the oocyte surface in a manner similar to the TZPs in OCGCs and *in vivo*-fully grown oocytes (Fig. 9, d1–g1). The mean numbers of TZPs in DO+GCs and DO+early MGCs (70.9±3.8 and 68.8±3.1, respectively) were similar to the numbers in OCGCs (72.6±1.9) and *in vivo*-growing oocytes (81.1±2.5, Denudation 0 in Fig. 10), although it was smaller than that of *in vivo*-fully grown oocytes (90.2±2.5) (Fig. 10).

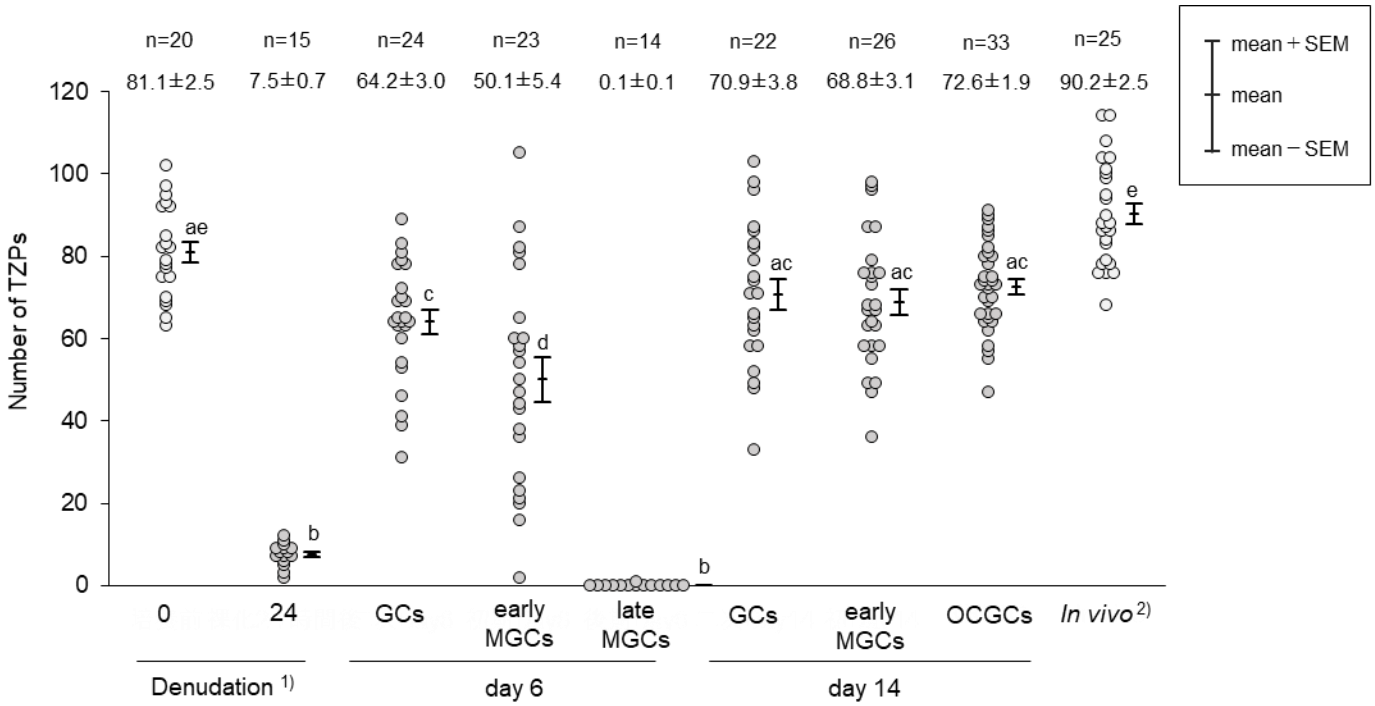

Figure 10 Changes in the number of TZPs in bovine oocytes in reconstructed complexes during *in vitro* growth culture. The number of visible actin-based TZPs that penetrated the zona pellucida to reach the oocyte surface was counted in the widest cross-section of the oocytes. The number of oocytes (n) used in each group and the mean (± SEM) number of TZPs are shown at the top. [1)] DOs collected from early antral follicles and cultured for 24 hours. [2)] *In vivo*-fully grown oocytes collected from late antral follicles. [a–e] Different letters denote significantly different values ($P < 0.05$).

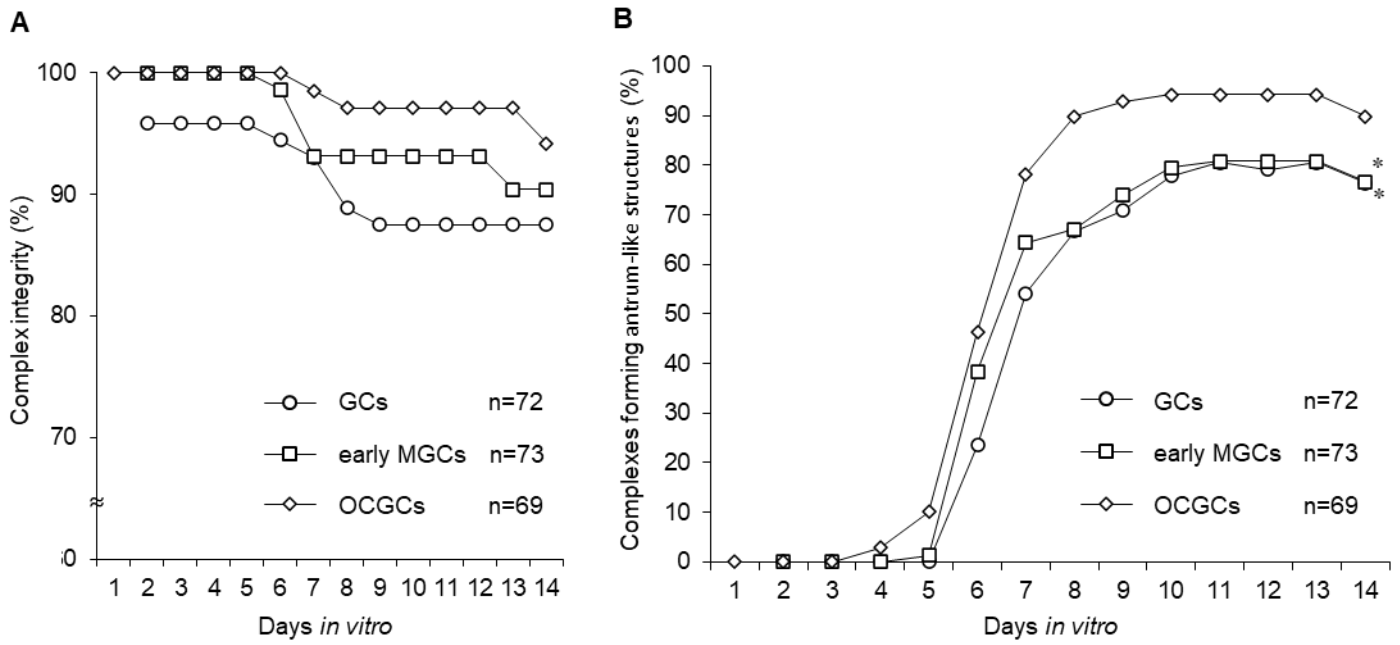

Figure 11 The integrity of reconstructed complexes and OCGCs (A) and formation of antrum-like structures by reconstructed complexes and OCGCs (B) during *in vitro* growth culture. GCs and early MGCs were cocultured with DOs. DO+GCs and DO+early MGCs were examined after starting the coculture. The numbers of complexes (n) used in each group are shown in each graph (A and B). * Values are significantly different from those of OCGCs ($P < 0.05$).

The mean diameters of oocytes grown in reconstructed complexes with GCs and early MGCs, and in OCGCs increased significantly (116.0±1.1 μm, 117.8±0.9 μm, and 119.0±0.8 μm, respectively) compared to oocytes before culture, although they were smaller than the size of *in vivo*-fully grown oocytes (126.5±0.5 μm) (Fig. 12).

After culture, 50% of the oocytes in DO+GCs, 74% of the oocytes in DO+early MGCs, and 69% of the oocytes in OCGCs reached the GV stage (Table 3). Growing oocytes collected from early antral follicles were at the FC or SC stages, while all *in vivo*-fully grown oocytes collected from late antral follicles were at the GV stage. In the subsequent maturation culture, 61%, 75%, and 71% of the oocytes in DO+GCs, DO+early MGCs, and OCGCs reached MII, respectively (Table 4). Most of the growing oocytes collected from early antral follicles remained at the FC stage after maturation culture, while all fully-grown oocytes collected from late antral follicles reached MII.

Transcriptome analysis of CCs, GCs, and MGCs

Since the culture experiments of DO+GC/MGC complexes suggested that late MGCs lost the ability to extend TZPs, transcriptome changes were analyzed among GCs, early MGCs, and late MGCs. CCs from early and late antral follicles (referred to as "early CCs" and "late CCs") were also subjected to the analysis.

First, the datasets from GCs, early CCs, late CCs, early MGCs, and late MGCs were analyzed using PCA and *t*-SNE dimensionality analysis, and visualized the expression of the marker genes (Fig. 13). PCA detected changes from GCs to early MGCs and late MGCs along the PC2 axis, while changes from GCs to late CCs along the PC1 axis (Fig. 13A). *t*-SNE analysis demonstrated that each type of the cells formed a cluster (Fig. 13B). Heatmap showed a distinct gene expression pattern in each cell group (Fig. 13C).

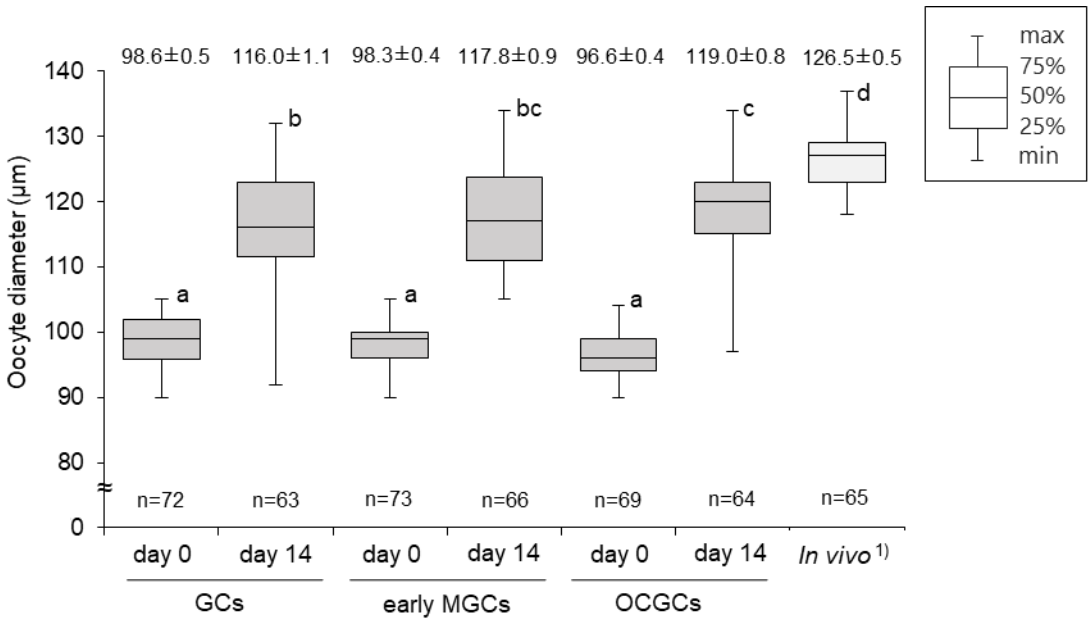

Figure 12 Diameters of bovine oocytes in reconstructed complexes after *in vitro* growth culture. DOs were cocultured with GCs and early MGCs. The number of oocytes (n) used in each group is shown at the bottom of each box. The mean (± SEM) diameters of oocytes are shown at the top of each box. [1)] The diameter of fully grown oocytes collected from late antral follicles (4–6 mm). [a-d] Different alphabets denote significantly different values ($P < 0.05$).

Table 3 Meiotic stages of *in vitro*-grown bovine oocytes in reconstructed complexes.

In vitro growth (day)	Types of complexes [1)]	Number of oocytes used	Number (%) of oocytes at each stage [4)]																	
			FC		SC		GV		ED		LD		MI		AI－TI		MII		DG	
0 [2)]	-	24	11	(46)	13	(54)	0	(0)	0	(0)	0	(0)	0	(0)	0	(0)	0	(0)	0	(0)
14	GCs	18	3	(17)	2	(11)	9	(50)	0	(0)	0	(0)	1	(6)	0	(0)	0	(0)	3	(17)
	early MGCs	19	0	(0)	1	(5)	14	(74)	0	(0)	1	(5)	0	(0)	0	(0)	0	(0)	3	(16)
	OCGCs	16	1	(6)	0	(0)	11	(69)	2	(13)	0	(0)	0	(0)	0	(0)	0	(0)	2	(13)
In vivo [3)]	-	20	0	(0)	0	(0)	20	(100)	0	(0)	0	(0)	0	(0)	0	(0)	0	(0)	0	(0)

[1)] Reconstructed complexes and OCGCs were subjected to *in vitro* growth culture. DOs were cocultured with GCs and early MGCs. [2)－4)] See the footnotes in Table 1.

Table 4 Meiotic competence of *in vitro*-grown bovine oocytes in reconstructed complexes after *in vitro* maturation.

In vitro growth (day)	Types of complexes [1)]	Number of oocytes used	Number (%) of oocytes at each stage [4)]																	
			FC		SC		GV		ED		LD		MI		AI − TI		MII		DG	
0 [2)]	-	16	13	(81)	0	(0)	0	(0)	0	(0)	0	(0)	1	(6)	0	(0)	0	(0)	2	(13)
14	GCs	18	1	(6)	0	(0)	0	(0)	0	(0)	0	(0)	6	(33)	0	(0)	11	(61)	0	(0)
	early MGCs	20	0	(0)	0	(0)	0	(0)	0	(0)	0	(0)	4	(20)	0	(0)	15	(75)	1	(5)
	OCGCs	14	0	(0)	0	(0)	0	(0)	0	(0)	0	(0)	3	(21)	0	(0)	10	(71)	1	(7)
In vivo [3)]	-	20	0	(0)	0	(0)	0	(0)	0	(0)	0	(0)	0	(0)	0	(0)	20	(100)	0	(0)

[1)] Reconstructed complexes and OCGCs were subjected to *in vitro* maturation culture after *in vitro* growth culture. [2)–4)] See the footnotes in Table 1.

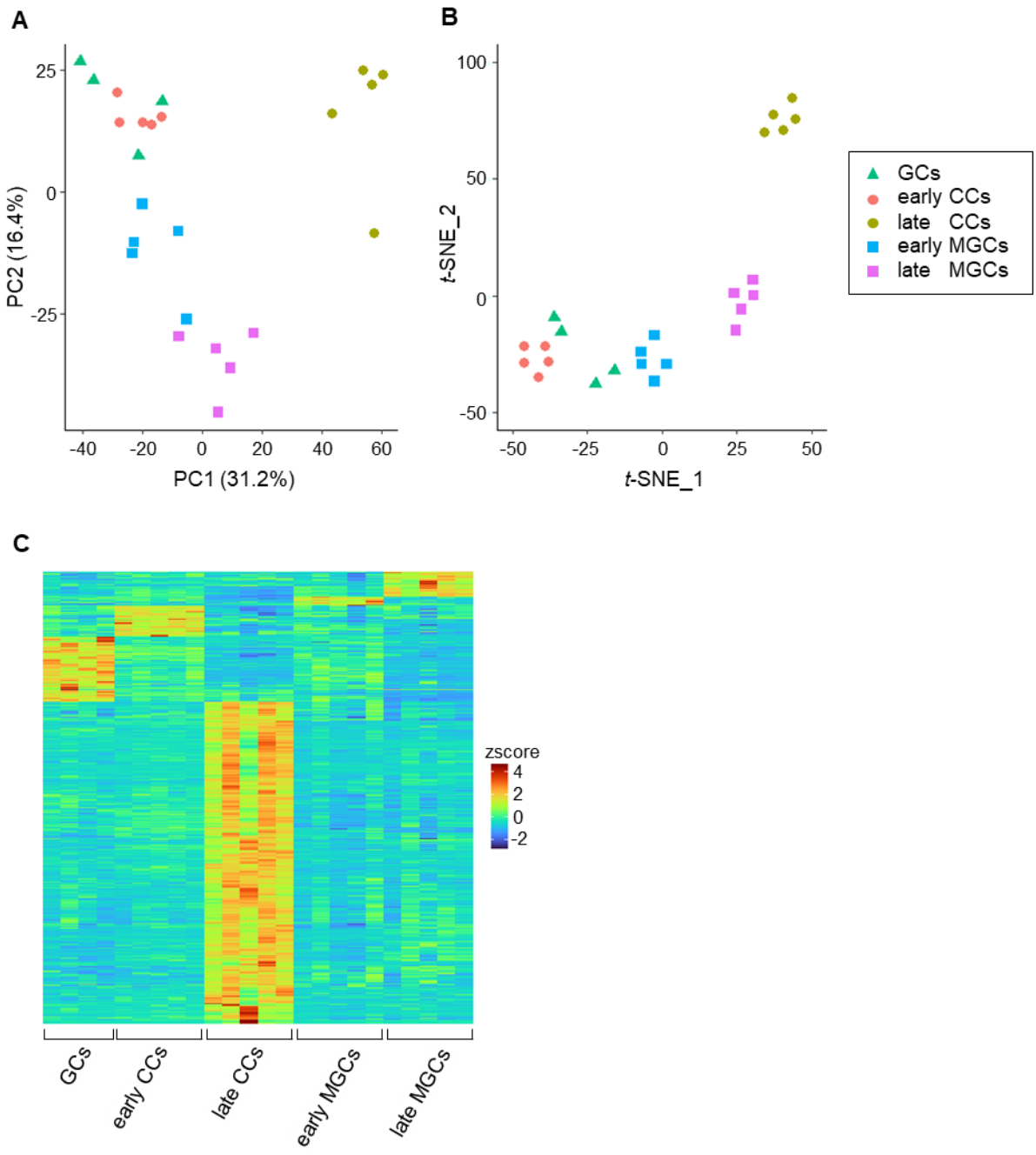

Figure 13 PCA plot (A), *t*-SNE plot (B), and heatmap visualizing the marker gene expression (C) using the datasets from bovine GCs, early CCs, late CCs, early MGCs, and late MGCs. Four GCs collected from secondary follicles, and five CCs and five MGCs each collected from early and late antral follicles were analyzed.

Based on these results, the transcriptome was analyzed by comparing the TZP generation group (GCs, early CCs, and early MGCs) with the non-TZP generation group (late MGCs). In the top 50 marker genes of the TZP generation group and the non-TZP generation group (Table 5, 6), *TLE6* (TLE family member 6, subcortical maternal complex member) and *CORO6* (coronin 6), which are involved in F-actin formation, and *SKAP2* (src kinase associated phosphoprotein 2), which is involved in the inhibition of actin polymerization, were included. The expression of *TLE6* decreased in late MGCs, and the expression of *CORO6* decreased toward late follicle stages (Fig. 14). In contrast, the expression of S*KAP2* increased toward late follicle stages. The expression of *DAAM1*, *FSCN1*, and *MYO10*, which are involved in filopodium formation (El-Hayek *et al*., 2018), was also examined. The expression of *FSCN1* and *MYO10* decreased in late MGCs. However, the expression of *DAAM1* did not decrease in late MGCs.

The GO analysis of DEGs revealed distinct characteristics in transcriptomes between the TZP generation group and the non-TZP generation group (Fig. 15). Comparing the datasets of the TZP generation group to those of the non-TZP generation group, a substantial number of DEGs were detected (up-regulated genes: n = 1,943; down-regulated genes: n = 1,716). Figure 16A showed that genes involved in the "cytoplasm" were mainly up-regulated in the TZP generation group. In addition, genes involved in "extracellular space and region", "membrane", and "secretory granule" were also up-regulated. In contrast, genes involved in "nucleolus" and "cytosol" were mainly down-regulated in the TZP generation group (Fig. 16B).

Table 5 The top 50 marker genes of the TZP generation group (GCs, early CCs, and early MGCs).

Rank	Gene symbol	Gene full name
1	NKD1	NKD inhibitor of WNT signaling pathway 1
2	CXCL3	chemokine (C-X-C motif) ligand 3
3	ENSBTAG00000051587	None
4	ALDH1A2	aldehyde dehydrogenase 1 family member A2
5	bta-mir-2887-1	bta-mir-2887-1
6	PLAC1	placenta enriched 1
7	EXOC3L1	exocyst complex component 3 like 1
8	TMEM163	transmembrane protein 163
9	CLSTN3	calsyntenin 3
10	TMEM59L	transmembrane protein 59 like
11	RGS4	regulator of G protein signaling 4
12	COLEC11	collectin subfamily member 11
13	**TLE6**	**TLE family member 6, subcortical maternal complex member**
14	SFRP4	secreted frizzled related protein 4
15	PDGFA	platelet derived growth factor subunit A
16	C8G	complement C8 gamma chain
17	SLC9A3R2	SLC9A3 regulator 2
18	METRN	meteorin, glial cell differentiation regulator
19	ENSBTAG00000048909	None
20	HEYL	hes related family bHLH transcription factor with YRPW motif like
21	PDGFB	platelet derived growth factor subunit B
22	KRT85	keratin 85
23	CLMP	CXADR like membrane protein
24	SASH1	SAM and SH3 domain containing 1
25	FLT1	fms related receptor tyrosine kinase 1
26	PHEX	phosphate regulating endopeptidase homolog X-linked
27	DMRTA1	DMRT like family A1
28	BEND6	BEN domain containing 6
29	ENSBTAG00000053867	None
30	SPARCL1	SPARC like 1
31	NPDC1	neural proliferation, differentiation and control 1
32	GRB7	growth factor receptor bound protein 7
33	ENHO	energy homeostasis associated
34	AMHR2	anti-Mullerian hormone receptor type 2
35	**CORO6**	**coronin 6**
36	PPFIA3	PTPRF interacting protein alpha 3
37	ENSBTAG00000032687	None
38	CTNND2	catenin delta 2
39	PRKCB	protein kinase C beta
40	PGAM2	phosphoglycerate mutase 2
41	DHH	desert hedgehog signaling molecule
42	ZCWPW1	zinc finger CW-type and PWWP domain containing 1
43	AXIN2	axin 2
44	SEPTIN5	septin 5
45	PCSK1N	proprotein convertase subtilisin/kexin type 1 inhibitor
46	CDH13	cadherin 13
47	CFAP161	cilia and flagella associated protein 161
48	KRT73	keratin 73
49	MESP1	mesoderm posterior bHLH transcription factor 1
50	TSPAN19	tetraspanin 19

The gene symbol and full name involved in F-actin formation are shown in bold.

Table 6 The top 50 marker genes of the non-TZP generation group (late MGCs).

Rank	Gene symbol	Gene full name
1	NFIA	nuclear factor I A
2	ENSBTAG00000002009	None
3	ENSBTAG00000038064	None
4	PCDH7	protocadherin 7
5	PPP1R14A	protein phosphatase 1 regulatory inhibitor subunit 14A
6	CPED1	cadherin like and PC-esterase domain containing 1
7	DKK3	dickkopf WNT signaling pathway inhibitor 3
8	**SKAP2**	**src kinase associated phosphoprotein 2**
9	ITGB8	integrin subunit beta 8
10	ENSBTAG00000015260	None
11	ENSBTAG00000051376	None
12	PIGW	phosphatidylinositol glycan anchor biosynthesis class W
13	ENSBTAG00000047030	None
14	RNASET2	ribonuclease T2
15	PLCB1	phospholipase C beta 1
16	ENSBTAG00000023318	None
17	MAN2A1	mannosidase alpha class 2A member 1
18	AMMECR1	AMMECR nuclear protein 1
19	GALNT7	polypeptide N-acetylgalactosaminyltransferase 7
20	ATP6V0A2	ATPase H+ transporting V0 subunit a2
21	SLC29A1	solute carrier family 29 member 1
22	DDAH1	dimethylarginine dimethylaminohydrolase 1
23	B4GALT6	beta-1,4-galactosyltransferase 6
24	F2R	coagulation factor II thrombin receptor
25	VKORC1L1	vitamin K epoxide reductase complex subunit 1 like 1
26	ENSBTAG00000039440	None
27	PCSK7	proprotein convertase subtilisin/kexin type 7
28	CDC123	cell division cycle 123
29	PARP14	poly(ADP-ribose) polymerase family member 14
30	RBM28	RNA binding motif protein 28
31	METTL13	methyltransferase 13, eEF1A lysine and N-terminal methyltransferase
32	ARSB	arylsulfatase B
33	MGST1	microsomal glutathione S-transferase 1
34	GPATCH4	G-patch domain containing 4
35	RASSF3	Ras association domain family member 3
36	SORBS2	sorbin and SH3 domain containing 2
37	MRS2	magnesium transporter MRS2
38	PDSS1	decaprenyl diphosphate synthase subunit 1
39	GUSB	glucuronidase beta
40	PPP2R1B	protein phosphatase 2 scaffold subunit Abeta
41	PDZD8	PDZ domain containing 8
42	DESI2	desumoylating isopeptidase 2
43	ENSBTAG00000051647	None
44	NAA15	N-alpha-acetyltransferase 15, NatA auxiliary subunit
45	ENSBTAG00000023823	None
46	DDX21	DExD-box helicase 21
47	RESF1	retroelement silencing factor 1
48	CCDC47	coiled-coil domain containing 47
49	IDE	insulin degrading enzyme
50	PINX1	PIN2 (TERF1) interacting telomerase inhibitor 1

The gene symbol and full name involved in F-actin formation are shown in bold.

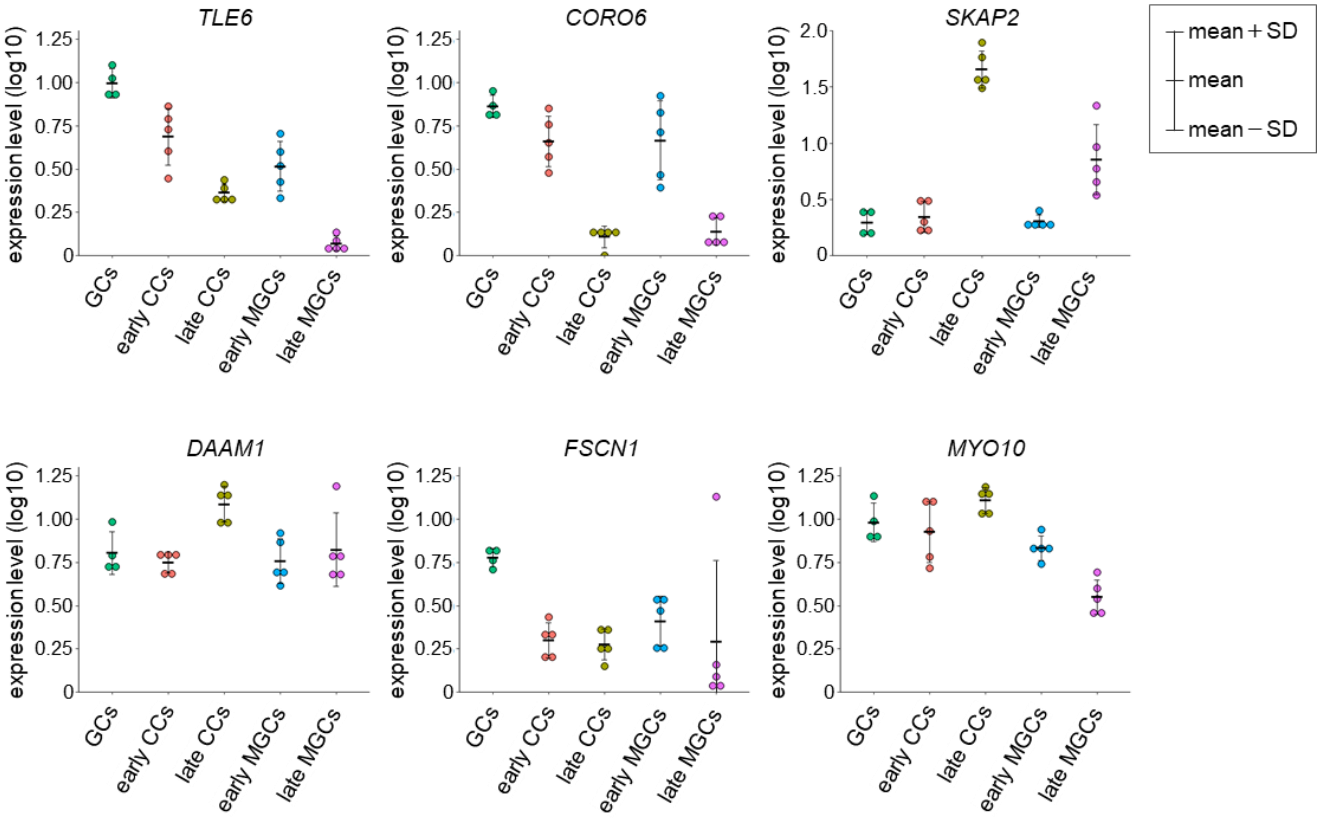

Figure 14 The gene expression in GCs, early CCs, late CCs, early MGCs, and late MGCs. The expression of genes involved in F-actin formation (*TLE6*, *CORO6*, *SKAP2*), and genes involved in filopodium formation (*DAAM1*, *FSCN1*, *MYO10*) are shown. The expression level is converted to $\log_{10}$ scale.

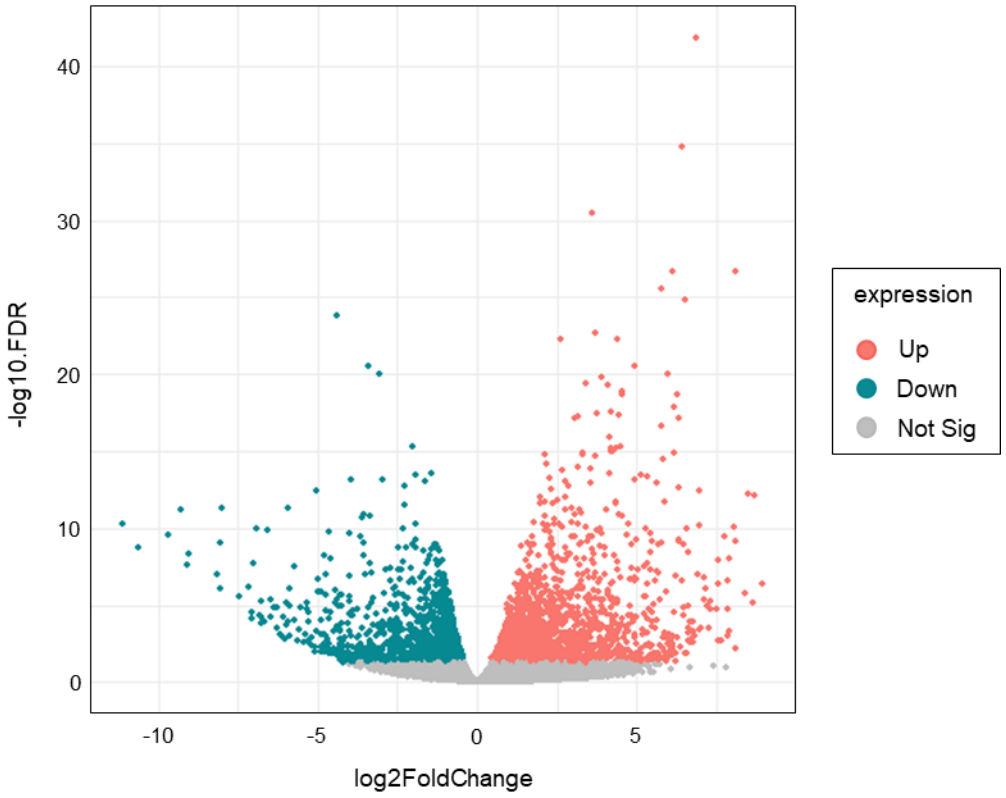

Figure 15 MA-plot of the datasets of the TZP generation group and the non-TZP generation group. Points are genes, x-axis indicates the $\log_2$ fold change, and the y axis indicates the $-\log_{10}$ FDR. Up-regulated genes (FDR < 0.05; $\log_2$ fold change > 0, n = 1,943) are marked in red, and down-regulated genes (FDR < 0.05; $\log_2$ fold change < 0, n = 1,716) are marked in blue.

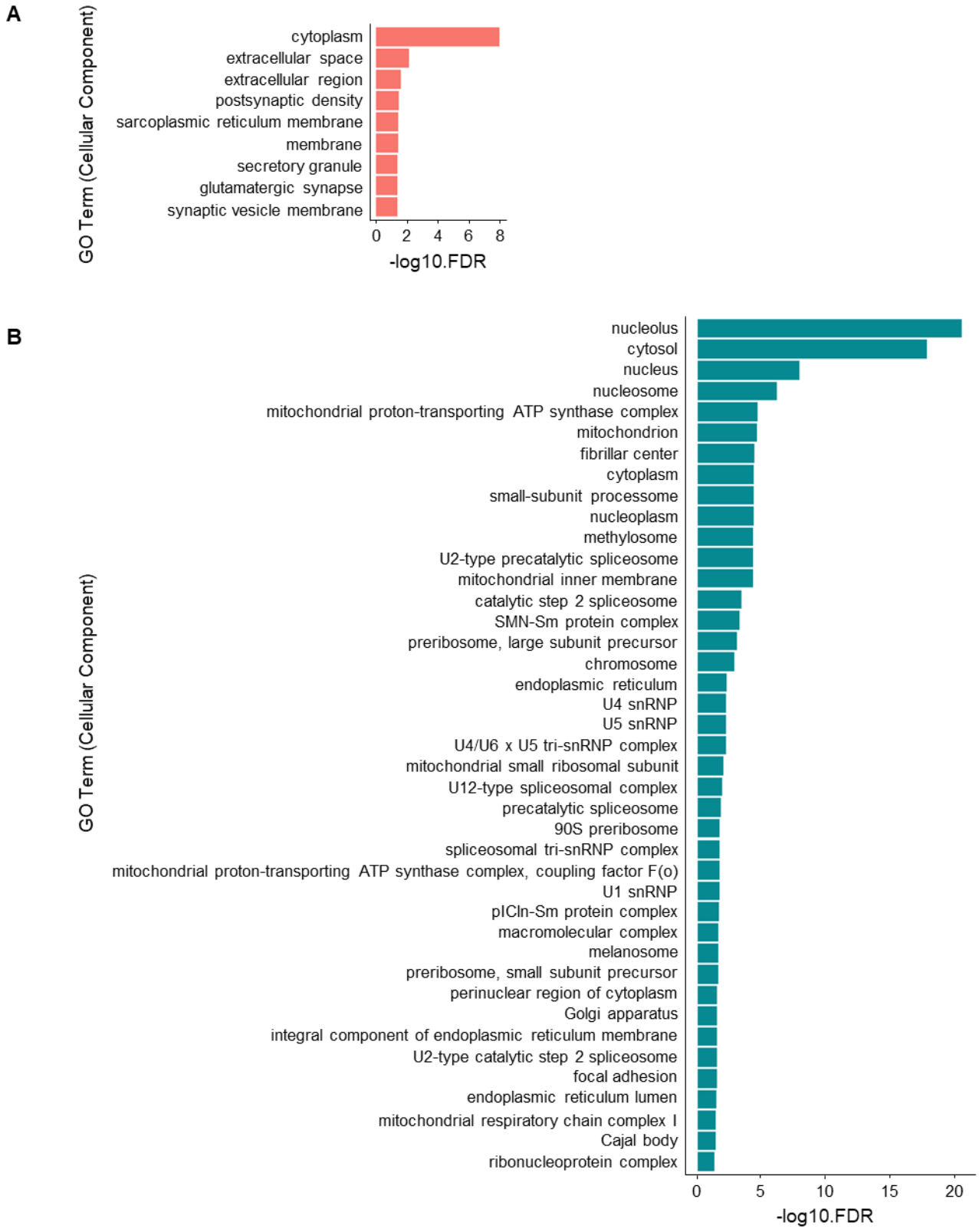

Figure 16 Representative GO terms of up-regulated (A) and down-regulated (B) enrichment between the TZP generation group and the non-TZP generation group. Up-regulated genes (FDR < 0.05; $\log_2$ fold change > 0, n = 1,943) and down-regulated genes (FDR < 0.05; $\log_2$ fold change < 0, n = 1,716) were analyzed.

Discussion

After coculture, GCs and early MGCs adhered to the DOs, and complexes were reconstructed. On day 6, regenerated TZPs were observed in oocytes cultured with GCs and early MGCs. In contrast, late MGCs barely adhered to the DOs and aggregated solidly, and regenerated TZPs were hardly observed in the complexes. These results suggest that late MGCs have little or no ability to extend TZPs. Since it was difficult to separate late MGCs from aggregated complexes by pipetting as opposed to GCs and early MGCs, the characteristic of late MGCs seems to be different from that of GCs and early MGCs. Considering that oocyte-derived factors induce CC phenotype (Eppig, 2001; Juengel and McNatty, 2005), it is supposed that late MGCs located far away from the oocytes are not affected by oocyte-derived factors in comparison with early MGCs. There is another possibility that the extracellular matrix (ECM) affects GC, CC, and MGC phenotypes (Hwang *et al*., 2000; Woodruff and Shea, 2007). When late MGCs were collected from late antral follicles, these cells constructed more rigid sheet-like structures than early MGCs. As the ECM component changes during follicle development (Woodruff and Shea, 2007), the MGC phenotype might be changed.

When the growth culture was continued until day 14, DO+GCs and DO+early MGCs developed similarly to OCGCs, even though the integrity of DO+GCs and DO+early MGCs during growth culture was lower than that of OCGCs. Although antrum formation in DO+GCs and DO+early MGCs occurred later than in OCGCs, they also formed antrum-like structures. Alam *et al*. (2018b) have proposed that GDF9 and BMP15 produced by bovine oocytes are involved in the formation of antrum-like structures. Therefore, the DOs in reconstructed complexes may have the ability to communicate with GCs and early MGCs to promote the formation of antrum-like structures in a manner similar to that of OCGCs. Interestingly, GCs that were collected from pre-antral follicles also formed antrum-like structures. In mice, oocytes

collected from secondary follicles accelerate the differentiation of GCs in primordial follicles and the rate of follicle development (Eppig *et al*., 2002). In the present study, GCs might be promoted to differentiate into CCs and MGCs by the oocytes collected from further-developed early antral follicles.

After culture, the mean numbers of TZPs in DO+GCs and DO+early MGCs increased until they became similar to those in OCGCs. TZPs probably develop simultaneously as the complexes develop. Although the mean numbers of TZPs in DO+GCs and DO+early MGCs were significantly lower than that in fully grown oocytes *in vivo*, the mean diameters of oocytes in DO+GCs and DO+early MGCs reached more than 115 µm. In addition, more than half of oocytes in DO+GCs and DO+early MGCs adequately progressed to GV stage and matured to MII after maturation culture. These percentages of the oocytes were lower in DO+GCs. Since GCs and DOs were collected from different sized follicles, bidirectional communication between these cells might not work well in some complexes. However, considering that CCs provide nutrients for oocyte growth and regulate cGMP levels for meiotic arrest through TZPs (Clarke, 2018a, 2018b), the regenerated TZPs by GCs and early MGCs are able to support oocyte growth. These results suggest that GCs became CC-like cells similar to early MGCs, and the regenerated TZPs were functional.

The transcriptome analysis shows that GCs clearly change in two directions into CCs and MGCs during follicle development. In addition, each cell group forms a cluster and has a distinct gene expression pattern. These results suggest that early MGCs and late MGCs are different cell types, which coincides with the change in the ability of MGCs to extend TZPs. Comparing the TZP generation group (GCs, early CCs, and early MGCs) with the non-TZP generation group (late MGCs), I focused on *TLE6*, *CORO6*, and *SKAP2* in the top 50 marker genes of each group. *TLE6* is known as one of the components of the subcortical maternal complex (SCMC) (Bebbere *et al*., 2016, 2021; Lu *et al*., 2017). SCMC is functionally conserved

in mammals and involved in diverse processes during the oocyte to embryo transition. In mice, the absence of maternal *TLE6* causes a lack of cytoplasmic F-actin meshwork formation and leads to asymmetric cell cleavage (Yu *et al.*, 2014). Coronins are a conserved family of actin cytoskeleton regulators, and involved in cell morphogenesis, cell migration, and endocytosis (Uetrecht and Bear, 2006; Chan *et al.*, 2011). *CORO6* is reported as a critical regulator for the stabilization of acetylcholine receptors clustering at the neuromuscular junction by modulating the actin cytoskeleton (Chen *et al.*, 2014). In contrast, *SKAP2* is indicated as an inhibitor of actin polymerization by interacting with actin assembly factors (Shimamura *et al.*, 2013). In mouse oocytes, lack of *SKAP2* causes failure of actin assembly, spindle migration, polar body extrusion, and asymmetric cytokinesis (He *et al.*, 2017). In the present study, the expression of *TLE6* and *CORO6* decreased, and the expression of *SKAP2* increased in late MGCs. These expression changes seem to synchronize the loss of the ability of TZP regeneration. Interestingly, in late CCs, the expression level of *CORO6* decreased, and the expression level of *SKAP2* increased. It is assumed that late CCs may be in a state of acceptance to retract TZPs for ovulation (Abbassi *et al.*, 2021). Since the quantities of *DAAM1*, *FSCN1*, *MYO10* mRNA are correlated with the number and density of TZPs in mice (El-Hayek *et al.*, 2018), TZPs are considered filopodium-like structures (Clarke, 2022). It is also reported that the number of MYO10 foci corresponds to the number of actin-TZPs in mouse and human ovarian follicles (Granados-Aparici *et al.*, 2022). In the present results, the expression of *FSCN1* and *MYO10* seem to correspond to the ability of bovine TZP regeneration. Although the present study does not show clearly that these 6 genes are involved in TZP generation, it is suggested that some factors involved in F-actin formation other than filopodium formation are involved in TZP generation.

Comparing the datasets of the TZP generation group to those of the non-TZP generation group, the GO analysis of DEGs also indicates the change in transcriptomes. In the TZP generation group, genes involved in “cytoplasm”, “extracellular space and region”, “membrane”,

and “secretory granule” were up-regulated. In contrast, genes involved in “nucleolus” and “cytosol” were down-regulated. Until the early antral follicle stage, GCs, CCs, and MGCs might have a common characteristic that is related to the communications and interactions with the oocytes. As the follicles develop further, MGCs seem to participate in other functions that might be different from direct support to oocyte growth.

In conclusion, the results in this chapter show that GCs are able to reconstruct complexes with DOs and regenerate TZPs similar to early MGCs. In addition, the oocytes in integrally reconstructed complexes grow fully and acquire meiotic competence, suggesting that the regenerated TZPs are functional, and GCs and early MGCs become CC-like cells. In contrast, late MGCs have lost the ability to extend TZPs and support oocyte growth. This characteristic of TZP generation is coincident with transcriptome changes in two directions from GCs into CCs or MGCs.

CHAPTER V

General summary

In the mammalian ovary, oocytes are surrounded by GCs or CCs. GCs adhere directly to oocytes in the primordial follicles. As the follicles develop and the zona pellucida is formed, the surrounding GCs extend TZPs penetrating the zona pellucida to maintain contact with the oocytes. After antrum formation, GCs differentiate into CCs and MGCs. CCs surrounding the oocyte maintain contact with the oocyte *via* TZPs, while MGCs apart from the oocyte line the basement membrane of the antral follicle. Then, CCs and MGCs have different phenotypes and different roles in the follicle.

During the follicle development, oocytes grow to full size. For the oocyte growth, bidirectional communication between oocytes and GCs or CCs through paracrine signaling and gap junctions at the ends of TZPs is essential. Oocyte-derived growth factors regulate development and function of GCs, and nutrients and mRNA from GCs or CCs are transported to oocytes through TZPs. Therefore, the maintenance of functional TZPs is important for the successful growth of oocytes in the ovary, and in *in vitro* culture.

In *in vitro* growth of bovine oocytes, culture systems using follicles and OCGCs collected from early antral follicles have been developed. In the systems, the maintenance of functional interactions between oocytes and GCs or CCs, and the formation of antrum-like structures seem to be the keys to success in creating a suitable microenvironment for oocyte growth. The purpose of the present study was to clarify the ability of CCs or MGCs alone to support bovine oocyte growth *in vitro* with a particular focus on the formation of antrum-like structures and the generation of TZPs.

In Chapter II, I aimed to determine whether CCs alone would support the growth of oocytes from early antral follicles (0.5–0.7 mm in diameter). In addition, to assess the effect of

FSH on OCC development, OCCs were cultured with various concentrations of FSH (0, 1, 5, 10, and 50 mIU/mL) for 14 days. Irrespective of FSH supplementation to the culture medium, OCCs developed and formed antrum-like structures in which MGC-like cells formed the outer wall of the structures. After growth culture, oocytes cultured without FSH and with 1 mIU/mL FSH grew to similar sizes to those of *in vivo*-fully grown oocytes, and acquired meiotic competence at high rates. Although FSH accelerated the formation of antrum-like structures, high concentrations of FSH (5, 10, and 50 mIU/mL) were not suitable for oocyte growth. These results suggest that CCs become MGC-like cells to form antrum-like structures and fully support oocyte growth *in vitro*.

Reversely, in Chapter III, I aimed to determine whether MGCs would regenerate TZPs as GCs and CCs do. First, I confirmed the disappearance of TZPs after 24 hours of oocyte denudation. Then, I examined the regeneration of TZPs during the coculture of TZP-free DOs with MGCs from early antral follicles. As the cytoskeletons of TZPs are primarily composed of F-actin, regenerated TZPs were detected by phalloidin staining after coculture for 24, 48, 72, 96, and 120 hours. In addition, the effects of FSH (1 mIU/mL) on the reconstruction of complexes and the regeneration of TZPs were also examined. After coculture, MGCs adhered to TZP-free DOs to reconstruct complexes, and TZPs were regenerated from MGCs to reach the oocyte surface. The number of TZPs increased with the development of DO+MGCs. Without FSH, the number of TZPs in some oocytes after coculture for 72 hours became similar to that in *in vivo* oocytes. In contrast, FSH retarded the regeneration of TZPs by MGCs. These results suggest that MGCs become CC-like cells to regenerate TZPs, and FSH negatively affects TZP regeneration by the MGCs.

It has been thought that CCs and MGCs have different phenotypes and different roles in the follicle. However, in Chapters II and III, the results suggested that CCs and MGCs from early antral follicles became MGC-like cells and CC-like cells, respectively. Then, in Chapter IV, I examined whether GCs from secondary follicles and MGCs from late antral follicles were able to

reconstruct complexes with TZP-free DOs and regenerate TZPs similar to MGCs from early antral follicles. Furthermore, to confirm that the regenerated TZPs were functional, the development of reconstructed complexes and oocyte growth in the complexes were determined. Since the abilities to regenerate TZPs were different among the cells, the transcriptome was analyzed among GCs, CCs, and MGCs collected from secondary, early antral, and late antral follicles. After coculture, GCs were able to reconstruct complexes with DOs and regenerate TZPs similar to early MGCs. In addition, the oocytes in integrally reconstructed complexes grew fully and acquired meiotic competence, suggesting that the regenerated TZPs are functional. In contrast, late MGCs had lost the ability to extend TZPs. This characteristic of TZP generation is coincident with transcriptome changes in two directions from GCs into CCs or MGCs. These results suggest that GCs from secondary follicles are promoted to become CC-like cells similar to early MGCs by the oocytes collected from further-developed early antral follicles; however, MGCs from late antral follicles are different from these cells and not able to become CC-like cells in the culture condition.

In summary, until the early antral follicle stage, bovine GCs, CCs, and MGCs have a common characteristic to generate TZPs and form antrum-like structures for supporting oocyte growth *in vitro*. In addition, as the follicles develop, MGCs lose the ability to extend TZPs, and they seem to participate in other functions that might be different from direct support to oocyte growth.

Acknowledgments

I would like to express my gratitude to Emeritus Professor Takashi Miyano and Associate Professor Jibak Lee for their scholastic teaching, guidance, and encouragement for my study. Without their guidance and persistent help, this thesis would not have been possible.

I am deeply grateful to Professor Hiroshi Harayama and Professor Hideyuki Mannen for their valuable comments and suggestions on my study and manuscripts. I would like to greatly thank Assistant Professor Hirohisa Kyogoku for teaching me RNA sequencing analysis techniques and for his valuable suggestions on my study and manuscripts. I would like to thank Ms. Rie Yamada for her cooperation and help in my study.

I would like to express my appreciation to the staff of the Kobe-Branch, Animal Biotechnology Center, Livestock Improvement Association of Japan, for providing bovine ovaries. I acknowledge the help and cooperation of Dr. Tomoya Kitajima and Dr. Tappei Mishina, the laboratory for chromosome segregation, RIKEN Center for Biosystems Dynamics Research, for allowing me to use laboratory equipment and for giving me technical assistance.

I really appreciate the members of my laboratory for helping me. Lastly, I would like to thank my family for cheering me up.

References

Abbassi L, El-Hayek S, Carvalho KF, Wang W, Yang Q, Granados-Aparici S, Mondadori R, Bordignon V, Clarke HJ. Epidermal growth factor receptor signaling uncouples germ cells from the somatic follicular compartment at ovulation. *Nat Commun*. 2021; 12: 1438.

Alam MH, Lee J, Miyano T. Inhibition of PDE3A sustains meiotic arrest and gap junction of bovine growing oocytes in *in vitro* growth culture. *Theriogenology*. 2018a; 118: 110–8.

Alam MH, Lee J, Miyano T. GDF9 and BMP15 induce development of antrum-like structures by bovine granulosa cells without oocytes. *J Reprod Dev*. 2018b; 64: 423–31.

Alam MH, Miyano T. Interaction between growing oocytes and granulosa cells *in vitro*. *Reprod Med Biol*. 2019; 19: 13–23.

Albertini DF, Combelles CM, Benecchi E, Carabatsos MJ. Cellular basis for paracrine regulation of ovarian follicle development. *Reproduction*. 2001; 121: 647–53.

Amrani KE, Alanis-Lobato G, Mah N, Kurtz A, Andrade-Navarro MA. Detection of condition-specific marker genes from RNA-seq data with MGFR. *PeerJ*. 2019; 7: e6970.

Baena V, Terasaki M. Three-dimensional organization of transzonal projections and other cytoplasmic extensions in the mouse ovarian follicle. *Sci Rep*. 2019; 9: 1262.

Barrett SL, Shea LD, Woodruff TK. Noninvasive index of cryorecovery and growth potential for human follicles *in vitro*. *Biol Reprod*. 2010; 82: 1180–9.

Bebbere D, Albertini DF, Coticchio G, Borini A, Ledda S. The subcortical maternal complex: emerging roles and novel perspectives. *Mol Hum Reprod*. 2021; 27: gaab043.

Bebbere D, Masala L, Albertini DF, Ledda S. The subcortical maternal complex: multiple functions for one biological structure? *J Assist Reprod Genet*. 2016; 33: 1431–8.

Buratini J, Dellaqua TT, Canto MD, Marca AL, Carone D, Renzini MM, Webb R. The putative roles of FSH and AMH in the regulation of oocyte developmental competence: from fertility prognosis to mechanisms underlying age-related subfertility. *Hum Reprod Update*. 2022; 28: 232–54.

Carabatsos MJ, Elvin J, Matzuk MM, Albertini DF. Characterization of oocyte and follicle development in growth differentiation factor-9-deficient mice. *Dev Biol*. 1998; 204: 373–84.

Cayo-Colca IS, Yamagami Y, Phan TC, Miyano T. A combination of FSH and dibutyryl cyclic AMP promote growth and acquisition of meiotic competence of oocytes from early porcine antral follicles. *Theriogenology*. 2011; 75: 1602–12.

Chan KT, Creed SJ, Bear JE. Unraveling the enigma: progress towards understanding the coronin family of actin regulators. *Trends Cell Biol*. 2011; 21: 481–8.

Chen Y, Ip FCF, Shi L, Zhang Z, Tang H, Ng YP, Ye WC, Fu AKY, Ip NY. Coronin 6 regulates acetylcholine receptor clustering through modulating receptor anchorage to actin cytoskeleton. *J Neurosci*. 2014; 34: 2413–21.

Chen S, Zhou Y, Chen Y, Gu J. fastp: an ultra-fast all-in-one FASTQ preprocessor. *Bioinformatics*. 2018; 34: i884–90.

Clarke HJ. History, origin, and function of transzonal projections: the bridges of communication between the oocyte and its environment. *Anim Reprod*. 2018a; 15: 215–23.

Clarke HJ. Regulation of germ cell development by intercellular signaling in the mammalian ovarian follicle. *Wiley Interdiscip Rev Dev Biol*. 2018b; 7: 1–22.

Clarke HJ. Transzonal projections: essential structures mediating intercellular communication in the mammalian ovarian follicle. *Mol Reprod Dev*. 2022; 1–17.

Collado MD, Silveira JC, Sangalli JR, Andrade GM, Sousa LRS, Silva LA, Meirelles FV, Perecin F. Fatty acid binding protein 3 and transzonal projections are involved in lipid accumulation during *in vitro* maturation of bovine oocytes. *Sci Rep*. 2017; 7: 2645.

Combelles CMH, Carabatsos MJ, Kumar TR, Matzuk MM, Albertini DF. Hormonal control of somatic cell oocyte interactions during ovarian follicle development. *Mol Reprod Dev*. 2004; 69: 347–55.

Conti M, Hsieh M, Zamah AM, Oh JS. Novel signaling mechanisms in the ovary during oocyte maturation and ovulation. *Mol Cell Endocrinol*. 2012; 356: 65–73.

Das D, Arur S. Regulation of oocyte maturation: Role of conserved ERK signaling. *Mol Reprod*

Dev. 2022; 89: 353–74.

Diaz FJ, Wigglesworth K, Eppig JJ. Oocytes are required for the preantral granulosa cell to cumulus cell transition in mice. *Dev Biol*. 2007; 305: 300–11.

Edson MA, Nagaraja AK, Matzuk MM. The mammalian ovary from genesis to revelation. *Endocr Rev*. 2009; 30: 624–712.

El-Hayek S, Demeestere I, Clarke HJ. Follicle-stimulating hormone regulates expression and activity of epidermal growth factor receptor in the murine ovarian follicle. *Proc Natl Acad Sci USA*. 2014; 111: 16778–83.

El-Hayek S, Yang Q, Abbassi L, FitzHarris G, Clarke HJ. Mammalian oocytes locally remodel follicular architecture to provide the foundation for germline-soma communication. *Curr Biol*. 2018; 28: 1124–31.

Emori C, Ito H, Fujii W, Naito K, Sugiura K. Oocytes suppress FOXL2 expression in cumulus cells in mice. *Biol Reprod*. 2020; 103: 85–93.

Eppig JJ. Oocyte control of ovarian follicular development and function in mammals. *Reproduction*. 2001; 122: 829–38.

Eppig JJ, O'Brien MJ. Development *in vitro* of mouse oocytes from primordial follicles. *Biol Reprod*. 1996; 54: 197–207.

Eppig JJ, Pendola FL, Wigglesworth K, Pendola JK. Mouse oocytes regulate metabolic cooperativity between granulosa cells and oocytes: amino acid transport. *Biol Reprod*. 2005; 73: 351–7.

Eppig JJ, Wigglesworth K, Pendola FL. The mammalian oocyte orchestrates the rate of ovarian follicular development. *Proc Natl Acad Sci U S A*. 2002; 99: 2890–4.

Eppig JJ, Wigglesworth K, Pendola F, Hirao Y. Murine oocytes suppress expression of luteinizing hormone receptor messenger ribonucleic acid by granulosa cells. *Biol Reprod*. 1997; 56: 976–84.

Fair T, Hyttel P, Greve T. Bovine oocyte diameter in relation to maturational competence and transcriptional activity. *Mol Reprod Dev*. 1995; 42: 437–42.

Granados-Aparici S, Volodarsky-Perel A, Yang Q, Anam S, Tulandi T, Buckett W, Son WY, Younes G, Chung GT, Jin S, Terret ME, Clarke HJ. MYO10 promotes transzonal projection-dependent germ line-somatic contact during mammalian folliculogenesis. *Biol Reprod*. 2022; 107: 474–87.

Gutierrez CG, Campbell BK, Webb R. Development of a long-term bovine granulosa cell culture system: induction and maintenance of estradiol production, response to follicle-stimulating hormone, and morphological characteristics. *Biol Reprod*. 1997; 56: 608–16.

Gutierrez CG, Ralph JH, Telfer EE, Wilmut I, Webb R. Growth and antrum formation of bovine preantral follicles in long-term culture *in vitro*. *Biol Reprod*. 2000; 62: 1322–8.

Harada M, Miyano T, Matsumura K, Osaki S, Miyake M, Kato S. Bovine oocytes from early antral follicles grow to meiotic competence *in vitro*: effect of FSH and hypoxanthine. *Theriogenology*. 1997; 48: 743–55.

He SW, Xu BH, Liu Y, Wang YL, Chen MH, Xu L, Liao BQ, Lui R, Li FP, Lin YH, Fu XP, Fu BB, Hong ZW, Liu YX, Qi ZQ, Wang HL. SKAP2 regulates Arp2/3 complex for actin-mediated asymmetric cytokinesis by interacting with WAVE2 in mouse oocytes. *Cell Cycle*. 2017; 16: 2272–81.

Hikabe O, Hamazaki N, Nagamatsu G, Obata Y, Hirao Y, Hamada N, Shimamoto S, Imamura T, Nakashima K, Saitou M, Hayashi K. Reconstitution *in vitro* of the entire cycle of the mouse female germ line. *Nature*. 2016; 539: 299–303.

Hirao Y. Conditions affecting growth and developmental competence of mammalian oocytes *in vitro*. *Anim Sci J*. 2011; 82: 187–97.

Hirao Y. Isolation of ovarian components essential for growth and development of mammalian oocytes *in vitro*. *J Reprod Dev.* 2012; 58: 167–74.

Hirao Y, Itoh T, Shimizu M, Iga K, Aoyagi K, Kobayashi M, Kacchi M, Hoshi H, Takenouchi N. *In vitro* growth and development of bovine oocyte-granulosa cell complexes on the flat substratum: effects of high polyvinylpyrrolidone concentration in culture medium. *Biol Reprod*. 2004; 70: 83–91.

Hirao Y, Miyano T. *In vitro* oocyte development in large animals. *J Mamm Ova Res*. 2014; 31: 79–

85.

Hirao Y, Shimizu M, Iga K, Takenouchi N. Optimization of oxygen concentration for growing bovine oocytes *in vitro*: constant low and high oxygen concentrations compromise the yield of fully grown oocytes. *J Reprod Dev*. 2012; 58: 204–11.

Hirao Y, Tsuji Y, Miyano T, Okano A, Miyake M, Kato S, Moor RM. Association between $p34^{cdc2}$ levels and meiotic arrest in pig oocytes during early growth. *Zygote*. 1995; 3: 325–32.

Huang DW, Sherman BT, Tan Q, Collins JR, Alvord WG, Roayaei J, Stephens R, Baseler MW, Lane HC, Lempicki RA. The DAVID Gene Functional Classification Tool: a novel biological module-centric algorithm to functionally analyze large gene lists. *Genome Biol.* 2007; 8: R183.

Huang W, Kang SS, Nagai K, Yanagawa Y, Takahashi Y, Nagano M. Mitochondrial activity during pre-maturational culture in *in vitro*-grown bovine oocytes is related to maturational and developmental competences. *Reprod Fertil Dev*. 2016; 28: 349–56.

Hulshof SC, Figueiredo JR, Beckers JF, Bevers MM, van der Donk JA, van den Hurk R. Effects of fetal bovine serum, FSH and 17β-estradiol on the culture of bovine preantral follicles. *Theriogenology*. 1995; 44: 217–26.

Hummitzsch K, Anderson RA, Wilhelm D, Wu J, Telfer EE, Russell DL, Robertson SA, Rodgers RJ. Stem cells, progenitor cells, and lineage decisions in the ovary. *Endocr Rev*. 2015; 36: 65–91.

Hummitzsch K, Irving-Rodgers HF, Hatzirodos N, Bonner W, Sabatier L, Reinhardt DP, Sado Y, Ninomiya Y, Wilhelm D, Rodgers RJ. A new model of development of the mammalian ovary and follicles. *PLoS One*. 2013; 8: e55578.

Hwang DH, Kee SH, Kim K, Cheong KS, Yoo YB, Lee BL. Role of reconstituted basement membrane in human granulosa cell culture. *Endocr J*. 2000; 47: 177–83.

Hyttel P, Fair T, Callesen H, Greve T. Oocyte growth, capacitation and final maturation in cattle. *Theriogenology*. 1997; 47: 23–32.

Itoh T, Kacchi M, Abe H, Sendai Y, Hoshi H. Growth, antrum formation, and estradiol

production of bovine preantral follicles cultured in a serum-free medium. *Biol Reprod*. 2002; 67: 1099–105.

Jaffe LA, Egbert JR. Regulation of mammalian oocyte meiosis by intercellular communication within the ovarian follicle. *Annu Rev Physiol*. 2017; 79: 237–60.

Juengel JL, McNatty KP. The role of proteins of the transforming growth factor-β superfamily in the intraovarian regulation of follicular development. *Hum Reprod Update*. 2005; 11: 143–60.

Kim D, Langmead B, Salzberg SL. HISAT: a fast spliced aligner with low memory requirements. *Nat Methods*. 2015; 12: 357–60.

Krijthe JH. Rtsne: T-distributed stochastic neighbor embedding using a Barnes-Hut implementation. 2015; Available at: https://github.com/jkrijthe/Rtsne.

Li H, Handsaker B, Wysoker A, Fennell T, Ruan J, Homer N, Marth G, Abecasis G, Durbin R, 1000 Genome Project Data Processing Subgroup. The sequence alignment/map format and SAMtools. *Bioinformatics*. 2009; 25: 2078–9.

Li R, Albertini DF. The road to maturation: somatic cell interaction and self-organization of the mammalian oocyte. *Nat Rev Mol Cell Biol*. 2013; 14: 141–52.

Liao Y, Smyth GK, Shi W. featureCounts: an efficient general purpose program for assigning sequence reads to genomic features. *Bioinformatics*. 2014; 30: 923–30.

Lu X, Gao Z, Qin D, Li L. A maternal functional module in the mammalian oocyte-to-embryo transition. *Trends Mol Med*. 2017; 23: 1014–23.

Luciano AM, Franciosi F, Modina SC, Lodde V. Gap junction-mediated communications regulate chromatin remodeling during bovine oocyte growth and differentiation through cAMP-dependent mechanism(s). *Biol Reprod*. 2011; 85: 1252–9.

Macaulay AD, Gilbert I, Caballero J, Barreto R, Fournier E, Tossou P, Sirard MA, Clarke HJ, Khandjian EW, Richard FJ, Hyttel P, Robert C. The gametic synapse: RNA transfer to the bovine oocyte. *Biol Reprod*. 2014; 91: 1–12.

Macaulay AD, Gilbert I, Scantland S, Fournier E, Ashkar F, Bastien A, Shojaei Saadi HA,

Gagne D, Sirard MA, Khandjian EW, Richard FJ, Hyttel P, Robert C. Cumulus cell transcripts transit to the bovine oocyte in preparation for maturation. *Biol Reprod*. 2016; 94: 1–11.

Makita M, Miyano T. Steroid hormones promote bovine oocyte growth and connection with granulosa cells. *Theriogenology*. 2014; 82: 605–12.

Makita M, Miyano T. Androgens promote the acquisition of maturation competence in bovine oocytes. *J Reprod Dev*. 2015; 61: 211–7.

Makita M, Ueda M, Miyano T. The fertilization ability and developmental competence of bovine oocytes grown *in vitro*. *J Reprod Dev*. 2016; 62: 379–84.

Matzuk MM, Burns KH, Viveiros MM, Eppig JJ. Intercellular communication in the mammalian ovary: oocytes carry the conversation. *Science*. 2002; 296: 2178–80.

McLaughlin M, Bromfield JJ, Albertini DF, Telfer EE. Activin promotes follicular integrity and oogenesis in cultured pre-antral bovine follicles. *Mol Hum Reprod*. 2010; 16: 644–53.

Mishina T, Tabata N, Hayashi T, Yoshimura M, Umeda M, Mori M, Ikawa Y, Hamada H, Nikaido I, Kitajima TS. Single-oocyte transcriptome analysis reveals aging-associated effects influenced by life stage and calorie restriction. *Aging Cell*. 2021; 20: e13428.

Mizumachi S, Aritomi T, Sasaki K, Matsubara K, Hirao Y. Macromolecular crowded conditions strengthen contacts between mouse oocytes and companion granulosa cells during *in vitro* growth. *J Reprod Dev*. 2018; 64: 153–60.

Morikawa R, Kyogoku H, Lee J, Miyano T. Oocyte-derived growth factors promote development of antrum-like structures by porcine cumulus granulosa cells *in vitro*. *J Reprod Dev*. 2022; 68: 238–45.

Morikawa R, Lee J, Miyano T. Effects of oocyte-derived growth factors on the growth of porcine oocytes and oocyte-cumulus cell complexes *in vitro*. *J Reprod Dev*. 2021; 67: 273–81.

Motlík J, Koefoed-Johnsen HH, Fulka J. Breakdown of the germinal vesicle in bovine oocytes cultivated *in vitro*. *J Exp Zool*. 1978; 205: 377–83.

Muñoz EL, Fuentes FB, Felmer RN, Yeste M, Arias ME. Extracellular vesicles in mammalian reproduction: a review. *Zygote*. 2022; 30: 440–63.

Nagaoka SI, Saitou M. Reconstitution of female germ cell fate determination and meiotic initiation in mammals. *Cold Spring Harb Symp Quant Biol*. 2017; 82: 213–22.

Oi A, Tasaki H, Munakata Y, Shirasuna K, Kuwayama T, Iwata H. Effects of reaggregated granulosa cells and oocytes derived from early antral follicles on the properties of oocytes grown *in vitro*. *J Reprod Dev*. 2015; 61: 191–7.

Pepling ME, Spradling AC. Female mouse germ cells form synchronously dividing cysts. *Development*. 1998; 125: 3323–8.

Richani D, Gilchrist RB. The epidermal growth factor network: role in oocyte growth, maturation and developmental competence. *Hum Reprod Update*. 2018; 24: 1–14.

Richard S, Baltz JM. Prophase I arrest of mouse oocytes mediated by natriuretic peptide precursor C requires GJA1 (connexin-43) and GJA4 (connexin-37) gap junctions in the antral follicle and cumulus-oocyte complex. *Biol Reprod*. 2014; 90: 137.

Robinson MD, McCarthy DJ, Smyth GK. edgeR: a Bioconductor package for differential expression analysis of digital gene expression data. *Bioinformatics*. 2010; 26: 139–40.

Russell DL, Robker RL. Molecular mechanisms of ovulation: co-ordination through the cumulus complex. *Hum Reprod Update*. 2007; 13: 289–312.

Saitou M, Miyauchi H. Gametogenesis from pluripotent stem cells. *Cell Stem Cell*. 2016; 18: 721–35.

Saitou M, Yamaji M. Primordial germ cells in mice. *Cold Spring Harb Perspect Biol*. 2012; 4: a008375.

Senbon S, Miyano T. Bovine oocytes in early antral follicles grow in serum-free media: effect of hypoxanthine on follicular morphology and oocyte growth. *Zygote*. 2002; 10: 301–9.

Shimamura S, Sasaki K, Tanaka M. The Src substrate SKAP2 regulates actin assembly by interacting with WAVE2 and cortactin proteins. *J Biol Chem*. 2013; 288: 1171–83.

Simon AM, Goodenough DA. Diverse functions of vertebrate gap junctions. *Trends Cell Biol.* 1998; 8: 477–83.

Su YQ, Sugiura K, Eppig JJ. Mouse oocyte control of granulosa cell development and function: paracrine regulation of cumulus cell metabolism. *Semin Reprod Med*. 2009; 27: 32–42.

Su YQ, Sugiura K, Wigglesworth K, O'Brien MJ, Affourtit JP, Pangas SA, Matzuk MM, Eppig JJ. Oocyte regulation of metabolic cooperativity between mouse cumulus cells and oocytes: BMP15 and GDF9 control cholesterol biosynthesis in cumulus cells. *Development.* 2008; 135: 111–21.

Sugiura K, Pendola FL, Eppig JJ. Oocyte control of metabolic cooperativity between oocytes and companion granulosa cells: energy metabolism. *Dev Biol*. 2005; 279: 20–30.

Tam PP, Snow MH. Proliferation and migration of primordial germ cells during compensatory growth in mouse embryos. *J Embryol Exp Morphol*. 1981; 64: 133–47.

Teilmann SC. Differential expression and localisation of connexin-37 and connexin-43 in follicles of different stages in the 4-week-old mouse ovary. *Mol Cell Endocrinol*. 2005; 234: 27–35.

Tsuji T, Kiyosu C, Akiyama K, Kunieda T. CNP/NPR2 signaling maintains oocyte meiotic arrest in early antral follicles and is suppressed by EGFR-mediated signaling in preovulatory follicles. *Mol Reprod Dev*. 2012; 79: 795–802.

Uetrecht AC, Bear JE. Coronins: the return of the crown. *Trends Cell Biol*. 2006; 16: 421–6.

Veitch GI, Gittens JE, Shao Q, Laird DW, Kidder GM. Selective assembly of connexin37 into heterocellular gap junctions at the oocyte/granulosa cell interface. *J Cell Sci*. 2004; 117: 2699–707.

Wandji SA, Eppig JJ, Fortune JE. FSH and growth factors affect the growth and endocrine function *in vitro* of granulosa cells of bovine preantral follicles. *Theriogenology*. 1996; 45: 817–32.

Wang Y, Lv C, Huang HL, Zeng MH, Yi DJ, Tan HJ, Peng TL, Yu WX, Deng HW, Xiao HM. Influence of mouse defective zona pellucida in folliculogenesis on apoptosis of granulosa cells and developmental competence of oocytes. *Biol Reprod*. 2019; 101: 457–65.

Wigglesworth K, Lee KB, Emori C, Sugiura K, Eppig JJ. Transcriptomic diversification of developing cumulus and mural granulosa cells in mouse ovarian follicles. *Biol Reprod*. 2015; 92: 23, 1–14.

Woodruff TK, Shea LD. The role of the extracellular matrix in ovarian follicle development. *Reprod Sci*. 2007; 14: 6–10.

Yamamoto K, Otoi T, Koyama N, Horikita N, Tachikawa S, Miyano T. Development to live young from bovine small oocytes after growth, maturation and fertilization *in vitro*. *Theriogenology*. 1999; 52: 81–9.

Yoshino T, Suzuki T, Nagamatsu G, Yabukami H, Ikegaya M, Kishima M, Kita H, Imamura T, Nakashima K, Nishinakamura R, Tachibana M, Inoue M, Shima Y, Morohashi K, Hayashi K. Generation of ovarian follicles from mouse pluripotent stem cells. *Science*. 2021; 373: eabe0237.

Yu XJ, Yi Z, Gao Z, Qin D, Zhai Y, Chen X, Ou-Yang Y, Wang ZB, Zheng P, Zhu MS, Wang H, Sun QY, Dean J, Li L. The subcortical maternal complex controls symmetric division of mouse zygotes by regulating F-actin dynamics. *Nat Commun*. 2014; 5: 4887.

Zhang M, Su YQ, Sugiura K, Xia G, Eppig JJ. Granulosa cell ligand NPPC and its receptor NPR2 maintain meiotic arrest in mouse oocytes. *Science*. 2010; 330: 366–9.